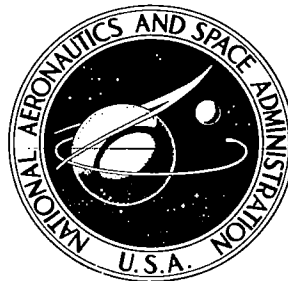


**NASA CONTRACTOR
REPORT**

NASA CR-1351



NASA CR-1351

201

0060440



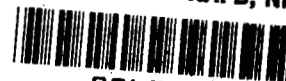
TECH LIBRARY KAFB, NM

LOAN COPY: RETURN TO
AFWL (WLIL-2)
KIRTLAND AFB, N MEX

DEVELOPMENT OF IMPEDANCE SIMULATION FIXTURES FOR SPACECRAFT VIBRATION TESTS

by Terry D. Scharton

Prepared by
BOLT BERANEK AND NEWMAN INC.
Van Nuys, Calif.
for Langley Research Center



NASA CR-1351

DEVELOPMENT OF IMPEDANCE SIMULATION FIXTURES
FOR SPACECRAFT VIBRATION TESTS

By Terry D. Scharton

Distribution of this report is provided in the interest of information exchange. Responsibility for the contents resides in the author or organization that prepared it.

Issued by Originator as BBN Report 1703

Prepared under Contract No. NAS 1-7600 by
BOLT BERANEK AND NEWMAN INC.
Van Nuys, Calif.

for Langley Research Center

NATIONAL AERONAUTICS AND SPACE ADMINISTRATION

ABSTRACT

An experimental program to develop vibration test fixtures which simulate the mount impedance of aerospace structures is conducted. Three fixtures designed to simulate the impedance of a launch vehicle are fabricated and evaluated in research vibration tests of a 1/2-scale mode Nimbus spacecraft. The results of the research tests indicate that impedance simulation fixtures eliminate some of the problems associated with conventional rigid fixtures at high frequencies. Guidelines for designing impedance simulation fixtures are presented.

TABLE OF CONTENTS

	<u>Page</u>
ABSTRACT	111
SUMMARY	1
INTRODUCTION	1
Conventional Test Fixture Problems	2
Simulation of Mounting Point Impedance	3
Multimodal Test Fixtures	4
Objectives of Investigation	5
SYMBOLS	5
DESIGN OF MULTIMODAL TEST FIXTURES	7
Average Point Impedance Simulation	7
Modal Enrichment	9
Effects of Damping	10
Development of 1/16 in. Multimodal Fixture	11
Development of Other Multimodal Fixtures	13
Fixture Design Guidelines	13
VIBRATION TEST RESULTS	15
Description of Test Configurations	16
Test Specification and Control	17
Transfer Functions in Sine-Sweep Tests	18
Transfer Functions in Octave-Band Random Tests	19
Effect of Excitation and Measurement Axes	21
Maximum Acceleration Levels Obtainable	22
SUBSTITUTE ACOUSTIC TEST RESULTS	23
Efficiency of Acoustical and Mechanical Excitation	23
Acoustic and Mechanical Excitation of Model Spacecraft	25
CONCLUSIONS AND RECOMMENDATIONS	26
REFERENCES	29

DEVELOPMENT OF IMPEDANCE SIMULATION FIXTURES FOR SPACECRAFT VIBRATION TESTS

By Terry D. Scharton
Bolt Beranek and Newman Inc.

SUMMARY

The use of conventional vibration test fixtures in aerospace system vibration tests often results in a number of test implementation problems and unrealistic vibration test data in the high-frequency regime. This report describes an experimental program to develop vibration test fixtures which simulate the mounting point impedance of aerospace vehicles to perform high-frequency vibration tests of spacecraft.

The report discusses the design, fabrication, and evaluation of a new "multimodal" type of vibration test fixture for performing high-frequency vibration tests. Vibration test data obtained in research tests with a 1/2-scale model Nimbus spacecraft suggests that the use of this type of fixture in future spacecraft programs would indeed eliminate many of the current high-frequency testing problems. The report presents guidelines for designing multimodal fixtures for future applications, and presents recommendations for additional research to further improve high-frequency vibration and shock testing technology.

INTRODUCTION

This investigation was motivated by a desire to develop a technique which would alleviate fixture resonance, over-testing, and response variation problems associated with the use of large conventional rigid test fixtures at high frequencies (approximately 100-2000 Hz). The testing technique investigated here is based on the concept of designing the test fixture in such a manner that it simulates, in an average sense, the point force impedance of the mounting structure adjacent to the spacecraft. (The point force impedance is the ratio of driving force to

the velocity response at a point when both force and velocity are sinusoidally varying with time at the same frequency.) In addition to the novel fixture concept, the testing technique developed involves a new and hopefully more realistic philosophy for specifying and controlling high-frequency spacecraft level vibration tests.

A related program (ref. 1) has also been conducted to develop an improved vibration testing technique for high-frequency spacecraft assembly-level tests. In that program an impedance simulation fixture was designed and evaluated in research tests of a model electronic assembly of the Mariner C spacecraft. The results of the program indicated that the novel fixture and testing technique resulted in a more realistic vibration environment on the assembly than conventional tests utilizing rigid assembly fixtures.

Conventional Test Fixture Problems

Figure 1 shows a 1/2-scale model Nimbus spacecraft mounted for a longitudinal vibration test on a conventional shaker-fixture configuration. This type of test configuration is commonly used to perform longitudinal sine-sweep and random vibration tests over the frequency range from 5 or 10 Hz to 2000 Hz or above. This type of test shaker-fixture configuration primarily simulates the low-frequency vibration environment associated with the fundamental vibration modes of the launch vehicle and spacecraft. When used at frequencies above approximately 100 Hz, this conventional type of test fixture often produces a number of annoying problems and produces unrealistic test results.

In spite of considerable effort to design vibration test fixtures as rigidly as possible, the first bending resonance of conventional fixtures often occurs within the frequency range of interest. For example, the fixture configuration shown in fig. 1 exhibits its first bending resonance at approximately 400 Hz, and the fixture used in the longitudinal tests of the full-scale Nimbus spacecraft conducted by the General Electric Company exhibits its first bending resonance at approximately 360 Hz.

Fixture resonances result in amplification of the fixture and spacecraft vibration levels and produce large spatial variations in the fixture vibration level, so

that it is difficult to measure a representative level which can be related to the test specification. In addition, stiff test fixtures designed to avoid the fixture resonance problem usually result in unrealistically high vibration transfer functions from the fixture into the spacecraft, because they do not simulate the mounting impedance of typical aerospace structures.

A number of brute force techniques have been developed to overcome the problems associated with the use of conventional fixtures in the high-frequency range. For example, expensive multichannel equalization equipment is utilized to "notch" (sharply decrease) the input vibration spectrum at fixture resonance frequencies to compensate for fixture resonance amplification, and it is becoming common practice to control the average of the fixture vibration levels at a number of mounting points in order to minimize the effects of spatial variation of the fixture response. At present, however, no technique is available for eliminating the high-frequency overtesting problem associated with the unrealistic impedance of rigid fixtures, although exploratory work has been conducted to utilize force, input power, or response control to minimize the overtesting problem.

A third problem area is associated with the unrealistic practice of performing high-frequency vibration tests along each of three perpendicular axes. It is common practice to require that the cross-axis fixture motion in these tests be limited to a small percentage, typically one percent, of the on-axis motion. This is a very difficult requirement to realize, and a great deal of effort and expense have been expended to develop very precise slip table configurations which will meet this requirement at frequencies as high as 2000 Hz.

Simulation of Mounting Point Impedance

Consideration of the difficulties encountered in utilizing conventional fixture configurations to simulate high-frequency vibration environments raises the question, "Are these difficulties associated with the basic objective of simulating high-frequency vibration environments, or are they associated primarily with the fact that current vibration testing techniques are based on a low-frequency philosophy?" In seeking an answer to this question, it

should be noted that structures resembling conventional fixtures and slip tables are not used in aerospace vehicles, and that inflight measurements rarely if ever indicate uniaxial vibration environments at 2000 Hz.

These considerations prompted this investigation of high-frequency vibration test fixtures which simulate the average impedance of aerospace mounting structures in order to eliminate the problems associated with conventional fixtures and provide a more realistic simulation of inflight high-frequency vibration environments.

It is appropriate at this point to discuss impedance simulation as used in this report. The Nimbus spacecraft is mounted on the Agena vehicle with a short conical section fabricated from 1/16 in. beryllium. Theoretically, it is possible to measure the point force and moment impedances (ref. 2) at each of the Nimbus-Agena interface points; and then build a hypothetical vibration test fixture which simulates the measured mounting point impedances. This would be a difficult task indeed. Alternatively, it is possible to construct a cylindrical structure which crudely resembles the forward section of the Agena vehicle and require that the point force impedance measured at some point on the surface of the cylindrical structure approximates the point force impedance of the Agena vehicle at some point removed from the mounting interface. It is also possible to go a step further and require not that the mounting structure simulates the impedance at a particular point on the Agena vehicle, but rather the average of the point force impedances measured at a large number of points on the forward section of the Agena vehicle. Simulation of the average impedance in this sense requires primarily that the cylinder radius, thickness, and material approximate the Agena vehicle. This investigation has followed the latter course, and a test fixture has been developed which crudely resembles the forward section of the Agena structure and simulates the average point impedance of the Agena skin.

Multimodal Test Fixtures

The impedance simulation fixtures developed in this program are typically much lighter in weight and more compliant than conventional test fixtures. These fixtures are used at frequencies well above their first resonance

frequency and exhibit many vibration resonances in order to simulate the high-frequency dynamic characteristics of the complete Agena vehicle. These fixtures are termed "multimodal fixtures" in order to distinguish them from conventional fixtures which operate below or in the vicinity of the first few resonance frequencies of the conventional fixtures.

Figure 2 shows the 1/2-scale model Nimbus spacecraft mounted on a multimodal fixture excited with three small 25-lb force shakers. The subsequent sections of this report discuss in detail the design, fabrication, and testing of this multimodal fixture.

Objectives of Investigation

The objectives of this investigation were:

- 1) To design and fabricate a multimodal fixture which realistically simulates the mounting impedance of an aerospace vehicle,
- 2) To determine the vibration characteristics of this fixture in sine-sweep and octave band tests,
- 3) To evaluate the feasibility of utilizing the multimodal fixture testing concept in future NASA spacecraft programs, and
- 4) To recommend problem and application areas associated with the multimodal fixture testing concept which require additional research and development.

SYMBOLS

a	radius of a cylinder
$\langle a_1^2 \rangle_{s,t}$	space-average mean-square multimodal fixture acceleration
$\langle a_2^2 \rangle_{s,t}$	space-average mean-square acceleration of the model spacecraft adapter
c_l	speed of compressional waves in a structure

f	frequency
f_r	ring frequency of a cylinder
f_o	modal resonance frequency
h	plate or cylinder thickness
A	plate or cylinder surface area
M	plate mass
M_1	mass of multimodal fixture
M_2	mass of model spacecraft adapter
P_1	power dissipated in multimodal fixture
P_{12}	power transmitted from the multimodal fixture to the spacecraft adapter
Y_o	point force admittance of a plate at position x_o and y_o
Y_∞	point force admittance of an infinite plate
$\delta(f)$	frequency separation between vibration resonances of a structure
$\delta_p(f)$	frequency separation of a flat plate
$\delta_{cyl}(f)$	frequency separation of a cylinder
δ_2	modal separation of the model spacecraft adapter
δ_1	modal separation of the multimodal fixture
η	damping loss factor
η_{12}	coupling loss factor from the multimodal fixture to the adapter
ρ_s	mass per unit area of a plate
Δ	half-power point bandwidth

DESIGN OF MULTIMODAL TEST FIXTURES

This section discusses the simulation of average point force impedance in detail, and describes the development of three multimodal test fixtures for conducting high-frequency vibration tests of the 1/2-scale model Nimbus spacecraft. Design guidelines and the general philosophy to be followed in designing a multimodal test fixture for high-frequency vibration tests of other spacecraft are also presented.

Average Point Impedance Simulation

To illustrate the concept of average point impedance simulation, consider the hypothetical case in which a test item is mounted at a point x_0 and y_0 on a finite rectangular plate (fig. 3A). The point force admittance (the reciprocal of impedance) at the point x_0, y_0 is defined as the velocity at the point when the plate is excited with a sinusoidal force of unity magnitude. The admittance as a function of frequency is obtained by performing a sine-sweep test with unit force input and measuring the velocity as a function of frequency. The real part of the admittance (defined as the component of velocity in phase with the exciting force) and the imaginary part of the admittance (defined as the component of velocity 90° out of phase with the exciting force) measured at a typical point on a plate is shown in fig. 3B.

The frequency separation between peaks in the real and imaginary parts of the point impedance is given by the modal separation $\delta(f)$. The modal separation (reciprocal of modal density [ref. 3]) for a simply supported plate is given by eq. 1

$$\delta_p(f) = \frac{hc_\ell}{\sqrt{3} A} \quad (1)$$

where A is the plate area, h the plate thickness, and c_ℓ the speed of compressional waves in the plate material (17,000 ft/sec for steel or aluminum). Thus for a 5 ft x 5 ft x 1/16 in. plate, the modal resonances occur approximately every 2 Hz. At frequencies above the first few resonances, eq. 1 is valid for a plate with arbitrary boundary conditions.

The peak-to-valley amplitude of the real and imaginary part of the point admittance is equal to $1/f\eta M$ where f is the excitation frequency, η is the damping loss factor which is equal to twice the damping ratio, and M is the total mass of the plate.

If an average point on the plate (averages over x_0 and y_0) is considered, the frequency averaged value of the real part of the admittance is equal to Y_∞ , the point force admittance of an infinite plate (ref. 4) which is given by eq. 2

$$Y_\infty = \sqrt{3}/4\rho_s hc_\ell \quad (2)$$

where ρ_s is the mass/unit area of the plate. The frequency average value of the imaginary part of the admittance is equal to zero.

If the point admittance is measured at a number of different points on the plate or at points on a number of different plates with slightly different shapes and boundary conditions, the measured impedances will vary slightly from that shown in fig. 3B. However the point force admittance (or impedance) of a plate can be simulated in an average sense by simulating:

- 1) the corresponding infinite plate force admittance given by eq. 2,
- 2) the corresponding plate modal separation given by eq. 1, and
- 3) the admittance peak-to-valley ration given by the product of the frequency, plate loss factor, and mass.

In this program a multimodal fixture has been designed which simulates in this average sense the mounting point impedance of the Agena skin. A cylindrical fixture fabricated from 1/16 in. steel sheet was constructed which simulates the average point impedance of the full-scale Agena vehicle skin, and a cylindrical fixture of 1/32 in. steel was constructed which simulates the point impedance of a 1/2-scale Agena vehicle.

Modal Enrichment

The modal separation of a cylindrical structure (ref. 3) is given by eq. 3

$$\delta_{\text{cyl}}(f) = \left(\frac{f_r}{f}\right)^{2/3} \frac{hc_l}{\sqrt{3} A}, \quad f < f_r \quad (3)$$

and $\delta_{\text{cyl}}(f) = \delta_p(f), \quad f > f_r$

where f_r is the ring frequency given by $f_r = 2\pi a/c_l$ where a is the cylinder radius. Since the modal separation of a cylindrical structure is inversely proportional to the cylinder area, it is necessary to artificially enrich the modal density of a small cylindrical fixture in order to simulate the modal separation and point impedance of a large aerospace vehicle.

In addition to its effect on the point impedance, the modal density of a structure is also important in determining the spatial and frequency variations in structural response. It has been shown (ref. 5) that for lightly damped structures, the spatial variations in the octave-band random response and sinesweep response and the frequency variations in the sinesweep response decrease as the number of vibration modes excited increase. Therefore it is desirable to enrich the modal density of a high-frequency test fixture even more than would be required to simulate the average point impedance of the mounting structure in order to reduce the frequency and spatial variations in the test fixture response and provide a more controlled vibration test.

Modal enrichment of a structure may be accomplished by attaching to the primary structure some secondary structure which exhibits a large number of vibration resonances in the frequency range of interest. Equation 1 indicates that if plate-like secondary structure is used to enrich modal density, the plates should be thin and have a large area. A second requirement for enriching modal density requires that the secondary structure have an impedance approximately equal to that of the primary structure and be relatively lightly damped in order that

the vibration modes of the secondary structure couple well to the primary structure and exhibit themselves in the primary structure response. Thus there is a trade-off which must be observed in selecting the secondary mode-enriching structure: The secondary structure must be thin and have large area in order to exhibit a large number of vibration modes, but the secondary structure must also be stiff enough to couple well to the primary structure. The results of a previous investigation (ref. 6) of the modal enrichment of a small plate indicates that wire-mesh constitutes an ideal modal enrichment secondary structure.

Effects of Damping

Damping also effects the point impedance of a structure and the spatial and frequency variations in the structure response. Figure 3 indicates that when the modal separation is large and the damping small so that the modal bandwidths (the half-power point band-width is defined as $\Delta = \eta f_0$, where f_0 is the resonance frequency) do not overlap in frequency, increasing the damping decreases the frequency variations in the impedance and the sine-sweep response. It has been shown however that when the modal separation is small and the modal damping large so that the modal bandwidths overlap in frequency, increasing the damping will not decrease the frequency variations in impedance and sine-sweep response and in fact will increase the spatial variations in the octave-band random response of the structure (ref. 5). Thus the optimum value of damping is approximately that which makes the modal bandwidth equal to the modal separation, eq. 4.

$$\eta(\text{optimum}) \approx \frac{\delta(f)}{f} \quad (4)$$

When a large structure is excited at several points with small shakers, the addition of large amounts of damping to the structure will also reduce the reverberant vibration levels on the structure and may result in significantly higher vibration levels in the vicinity of the shaker attachment points than at points far removed from the sources.

Development of 1/16 in. Multimodal Fixture

The bare 1/16 in. cylindrical fixture is shown in figs. 4A and B. The fixture consists of a 1/16 in. steel cylinder, 18 in. in height and 31 in. in diameter. A ring frame is attached inside the cylinder to support the adapter of the 1/2-scale model Nimbus spacecraft. In the development tests, the fixture was excited with three 25-lb force shakers attached along the cylinder radii as shown in fig. 4A.

The instrumentation used in the sine-sweep tests of the fixture is shown in fig. 5. In the open loop configuration, the three shakers are driven with a constant voltage sine wave, and the frequency is swept from 20 to 2000 Hz. The acceleration at a single point on the fixture is recorded on a graphic level recorder as a function of frequency. The sine-sweep response measured in the horizontal direction on the cylinder wall and the sine-sweep response in the vertical direction on the ring frame of the cylinder are shown in figs. 6A and B, respectively. The acceleration response is given on the right side of the figure in root-mean-square g's (g_{rms}) and on the left side of the figure in decibels defined as:

$$\text{Acceleration (dB)} = 20 \log_{10} (g_{rms})$$

The response plot in fig. 6A shows approximately seven response peaks between 0 and 200 cycles or an average modal separation of approximately 30 Hz which is to be compared with the theoretical value of 32 Hz at a frequency of 100 Hz calculated from eq. 3.

A number of configurations for enriching the modal density of the 1/16 in. cylinder shown in fig. 4 were investigated. In one configuration the cylinder was tightly packed with layers of 1 in. x 1/2 in. x 1/16 in. wire-mesh, in a second configuration the wire-mesh was replaced with four thin aluminum plates spaced inside the cylinder, and in a third configuration 18 platelike fins were attached along the radii inside the cylinder. The cylinder packed full of wire mesh exhibited a large number of vibration modes, but it was difficult to keep the mesh in place, and the packed mesh rattled and caused a nonlinear behavior. The two modifications involving thin plates did not show the desired modal enrichment.

The final configuration for enriching the modal density of the 1/16 in. cylinder is shown in fig. 7. In this configuration 18 horizontal coils of 1 in. x 1/2 in. x 1/16 in. wire-mesh are soldered to the ring frame, 18 vertical coils of wire-mesh are soldered to the cylinder walls, and three wire-mesh plates are soldered to the wire-mesh coils. In this configuration the wire-mesh increases the modal density without appreciably stiffening and inhibiting the low-frequency vibration modes of the cylinder. Figures 8A and B show the sine-sweep response on the cylinder wall and the ring frame of the enriched 1/16 in. cylinder. Comparison of these results with those shown for the bare cylinder, figs. 5A and B, indicates that the wire-mesh coils and plates significantly increase the modal density of the cylinder response at the low frequencies.

As the final step in the development of the 1/16 in. fixture a 1/16 in. layer of damping material (Lord Manufacturing Company LDS-501 sprayable damping material) was applied to the outer wall of the cylinder. The internal damping loss factors η of the bare and damped 1/16 in. cylinders are shown in fig. 9. Application of the damping material increased the damping loss factor by a factor of 2 or 3 over the entire frequency range of interest. The sine-sweep response of the enriched, damped 1/16 in. cylinder wall and ring frame are shown in figs. 10A and B, respectively. Comparison of figs. 10A and B with figs. 6A and B shows that the final 1/16 in. fixture configuration shows high modal density and relatively small peak-to-valley variation over the entire frequency range from 20 to 2000 Hz.

The instrumentation used in the octave-band random tests of the fixture is shown in fig. 11. The output of a white noise generator is filtered in a selected octave band, amplified and used to drive the three shakers attached to the fixture. The mean square acceleration at a point on the fixture is measured by passing the output of an accelerometer through the selected octave-band filter, averaging the filtered signal, and reading the level on a meter.

The measured normalized spatial variance of the random response (in decibels) of the enriched damped 1/16 in. fixture is shown in fig. 12. The response variance on the ring frame and on the cylinder wall are comparable.

Development of Other Multimodal Fixtures

A second multimodal fixture was developed utilizing a 1/32 in. thick cylinder as shown in fig. 13. Five wire mesh plates were added to enrich the modal density of the 1/32 in. cylinder. The sine-sweep response measured on the cylinder wall of the enriched 1/32 in. fixture is shown in fig. 14A. The sine-sweep response indicates high modal density and peak-to-valley ratios comparable to those obtained with the enriched 1/16 in. cylinder (fig. 8A). The sine-sweep response of the enriched 1/16 in. cylinder with a 1/32 in. layer of damping material sprayed on the outer wall of the cylinder is shown in fig. 14B. The application of the damping compound significantly increased peak-to-valley variations in the frequency response and degraded the performance of the 1/32 in. fixture.

A third multimodal fixture configuration constructed completely of wire-mesh, fig. 15, was also investigated. This configuration showed performance characteristics similar to the 1/32 in. cylindrical fixture discussed in the previous paragraph. The addition of damping to the wire-mesh fixture also degraded its performance.

It is believed that with the proper amount of damping the performance of the 1/32 in. cylindrical fixture and the wire-mesh fixture would have been comparable or slightly better than that of the enriched damped 1/16 in. fixture configuration. However, the performance of the 1/16 in. fixture was considered adequate, and the scope of this program did not allow refining the 1/32 in. and the wire-mesh fixtures to their point of optimum design.

Fixture Design Guidelines

From the results of this and a previous investigation (ref. 1), some tentative design guidelines for constructing multimodal fixtures for high-frequency vibration tests of spacecraft can be formulated. The basic philosophy in designing a multimodal fixture is to build a fixture which simulates a section of the mounting structure adjacent to the test item. The question naturally arises, "How much of the mounting structure should the fixture physically resemble?" The following rule of thumb can be stated. Define a characteristic length equal to the characteristic dimension of the test-item mounting-structure interface. For

example, the characteristic dimension of the 1/2-scale model Nimbus spacecraft mounting equals the diameter of the spacecraft adapter. The multimodal fixture should model the mounting structure at least one characteristic length on all sides of the test item. Thus, the multimodal fixtures developed for the model Nimbus spacecraft physically resembles a section of the Agena vehicle approximately one diameter in length.

The multimodal fixture should simulate the structural characteristics which are important in determining the high frequency dynamics. One guideline for realizing this simulation is to design the multimodal fixture so that the point force impedance measured at a number of points on the fixture simulates in an average sense the point force impedance of the mounting structure. In the case of the model Nimbus spacecraft, we have chosen the fixture cylinder thickness and material so that the point impedance of an infinite plate constructed of this thickness and material would be equal to the point impedance of an infinite plate constructed from the Agena vehicle skin.

The major task in developing a small multimodal fixture which simulates a large mounting structure is the enrichment of the fixture modal density to simulate the modal density of the large structure. The secondary structure used to enrich the modal density of the basic fixture must be compliant in order to contribute high modal density and must be strongly coupled to the primary structure. In the case of the model Nimbus spacecraft, 1/16 in. wire-mesh proved the best compromise for enriching the modal density of the 1/16 in. basic fixture cylinder. The enrichment of the modal density of the multimodal fixture is basically a trial and error process, and therefore sine-sweep tests of the multimodal fixture should be conducted during its development to assess the modal richness, frequency variation, and spatial variation of the fixture response.

The optimum amount of damping of the fixture should be such as to approximately yield modal overlap as indicated by eq. 4. In general the damping should be applied to the basic fixture structure rather than to the secondary structure or the mode enriching effect of the secondary structure may be nullified.

Excitation of the multimodal fixture can be accomplished by attaching a number of small shakers to the multimodal fixture or by mounting the multimodal fixture on a large slip-table configuration, although the first configuration is preferred because the slip table will generally inhibit some modes of the multimodal fixture and the slip table resonances may transmit through the multimodal fixture. The number of small shakers used to excite the fixture must be sufficient to establish a spatially uniform response on the fixture. This requires that the reverberant vibration field associated with the resonant modes of the fixture be equal to or larger than the direct field which a single shaker would excite in an infinite structure. The number of shakers required to excite the fixture will of course be larger if the fixture is quite heavily damped.

The final question regarding the application of multimodal fixtures concerns the frequency range over which the multimodal test fixture will provide a realistic test. It is believed that the multimodal test fixture developed in this investigation provides a realistic test at frequencies above 50 or 100 Hz. In tests involving larger spacecraft, multimodal test fixtures can be developed to operate at significantly lower frequencies. The design guideline is that the multimodal test fixture must operate well above its first few resonance frequencies and exhibit sufficient modal density in the frequency range of interest in order to provide a relatively smooth frequency response and small spatial and frequency response variations.

Finally the multimodal test fixture must be sturdy enough to withstand the static loads and fatigue loads associated with the vibration tests. This requirement did not constitute a problem in the present investigation.

VIBRATION TEST RESULTS

In this section vibration configurations incorporating the 1/16 in. enriched, damped multimodal test fixture and the 1/2-scale model Nimbus spacecraft are described, methods of specifying and controlling multimodal vibration tests are discussed, transfer functions from the fixture to the model spacecraft measured in controlled sine-sweep and octave-band random tests are presented, the effect

of the excitation and measurement axes on the spacecraft response is discussed, and the maximum acceleration levels obtainable with small shaker excitation of the multimodal fixture is investigated.

Description of Test Configurations

Both sine-sweep and octave-band random tests are conducted. In the sine-sweep tests the instrumentation shown in fig. 5 is used to control the average of three accelerometers on the control surface and maintain the control acceleration at a constant level as the frequency is swept from 20 to 2000 Hz. In the octave-band random tests the instrumentation shown in fig. 11 is used to excite the structure with an octave-band of noise and the acceleration responses at a number of points on the exciting structure and the spacecraft components are measured. The sine-sweep tests are useful for assessing the frequency variations in the response at a single point on a spacecraft component, whereas the octave-band random tests are useful for defining the space-average and spatial variation in vibration level on a particular spacecraft component. In general, the transfer functions obtained in the octave-band random tests are more representative since they represent the average on the transfer functions between many different points.

Two series of tests are conducted with the 1/2-scale model spacecraft mounted on the enriched damped 1/16 in. multimodal fixture described previously. In the first series of tests, the fixture is excited with three small (25-lb force) shakers in the radial direction as shown in fig. 2. In the second series of tests, the 1/16 in. fixture is mounted on a conventional slip table attached to a large (30,000-lb force) electrodynamic shaker as shown in fig. 1. The slip table series of tests involves tests in the longitudinal and each of the two horizontal axes.

Three series of tests are also conducted with the 1/2-scale model spacecraft without the multimodal test fixture. The adapter of the 1/2-scale model Nimbus spacecraft is very thin (two hundredths of an inch, approximately) and in itself constitutes a multimodal fixture. (In fact, the model spacecraft adapter is only 3/8th the thickness desired for 1/2-scale simulation (ref. 7).)

Therefore a series of tests is conducted utilizing three small shakers attached directly to the Nimbus adapter. In the second series of tests, the spacecraft adapter is attached directly to a conventional slip table and excited along each of three perpendicular axes. A final series of tests is conducted with the spacecraft adapter removed. In this final series, the ring frame of the spacecraft is attached directly to a slip table and excitation is provided along each of three perpendicular axes. These tests are conducted in order to obtain results for comparing multimodal fixture test results with the results of conventional slip table tests utilizing a large shaker.

Test Specification and Control

The philosophy for specifying and controlling the input vibration environment in multimodal fixture tests is quite different than that utilized in conventional slip table tests. In multimodal fixture tests the space-average vibration environment on the fixture is controlled rather than the vibration environment at a single point or at a number of points on the slip table spacecraft interface. This method for controlling multimodal fixture vibration tests is analogous to the method for specifying and controlling reverberant acoustic tests.

In reverberant acoustic tests, one places the test item in a large room containing a reverberant sound field and specifies the space-average pressure level far removed from the test item, rather than the pressure at the surface of the test item. The pressure at the surface of a typical test structure varies a great deal from point to point and depends upon the exact details of the structural surface. Similarly the vibration level at the interface of a slip table and a vibration test structure depends upon the details of the test structure mounting and at high frequencies exhibits large variations from point to point on the slip-table test structure interface.

Interface vibration measurements are also undesirable because it is hard to obtain a representative definition of an interface vibration measurement from flight data. Slight changes in the spacecraft weight or mounting configuration can have a large effect on the interface levels. However the reverberant vibration levels measured on the space vehicle somewhat removed from the interface remain

relatively constant from flight to flight and thus constitute a definable and representative vibration environment.

Transfer Functions in Sine-Sweep Tests

The sine-sweep tests conducted with the multimodal fixture and spacecraft mounted on the conventional rigid fixture as shown in fig. 1 indicate the severity of the fixture resonance problem associated with conventional fixtures. The vibration level at a single point on the fixture is controlled at a level of $1/2$ "g" rms over the frequency range from 20 to 2000 Hz. The response in the longitudinal excitation conventional test at one of the points where the multimodal fixture attaches to the fixture is shown in fig. 16A. This data clearly shows the effect of the first bending resonance of the fixture which results in an amplification of approximately 300 in the mean-square acceleration at the multimodal fixture mounting foot at a frequency of 420 Hz, and the data also indicate higher order fixture resonances at frequencies above 400 Hz. Figure 16A indicates that these resonances of the conventional fixture render the data essentially meaningless at frequencies greater than 300 Hz.

Figure 16B shows the sine-sweep response of the $1/2$ -scale model Nimbus solar panel in the same test. If one were not aware of the fixture resonance problems which exist at frequencies above 300 Hz, one might assume that the peak in the solar panel response at 400 Hz is associated with the dynamic characteristics of the solar panel and undertake a program to redesign or isolate the solar panel in order to eliminate the 400 cycle peak. Thus the resonances of the conventional large fixture used to couple the large shaker to the multimodal fixture exhibit themselves in the spacecraft response, and therefore it is recommended that a multiple small shaker scheme such as that shown in fig. 2 be utilized to excite multimodal fixtures.

The conventional slip table data obtained in horizontal axis tests of the model spacecraft do not exhibit severe fixture resonances. Figure 17A shows the fixture response at the control point in a horizontal excitation test, and fig. 17B shows the sine-sweep response at a single point on the enriched damped $1/16$ in. multimodal fixture in the same test. The gain from the slip table to the fixture is approximately 0 at 20 Hz and increases to approximately

5 dB at 2000 Hz. Comparison of figs. 17B and 10B indicates that the sine-sweep response of the multimodal fixture excited horizontally with the conventional slip-table and large-shaker configuration exhibits significantly larger frequency variations in the high-frequency regime than when the fixture is excited with three small shakers acting in the horizontal plane. Therefore small shaker excitation of the multimodal fixture is also more desirable than large shaker and slip table excitation of the multimodal fixture from the standpoint of reducing frequency variations in the multimodal fixture response.

Sine-sweep tests are also performed with the model Nimbus spacecraft mounted on a multimodal fixture excited with three small shakers as shown in fig. 2. The transfer functions measured in these sine-sweep tests are not presented in the report because the test results show very little information that is not contained in the octave-band transfer function based on space-average measurements which are presented in the next section.

Transfer Functions in Octave-Band Random Tests

Figure 18 presents the transfer function from the multimodal fixture to the spacecraft adapter in the octave-band random tests with three small shakers exciting the multimodal fixture and the transfer function from the conventional slip table to the adapter in tests with the spacecraft mounted on the large shaker as shown in fig. 1. The transfer function from the multimodal fixture to the adapter is equal to the ratio of the average of acceleration measurements at 6 points on the adapter to the average of acceleration measurements at 6 points on the multimodal fixture, and the transfer function from the slip table to the adapter is defined similarly. The data shown in fig. 18 indicate that the transfer function from the conventional slip table to the adapter is approximately 6 dB higher in the octave bands with center frequencies at 125 Hz and 250 Hz than the transfer function from the multimodal fixture to the adapter. In the high-frequency regime the transfer functions from the fixture and from the slip table to the adapter are approximately equal. The shaded range in the curves presented in fig. 18 indicate that the spatial standard deviations in the adapter responses in the two tests are approximately equal.

Figure 19 presents the space-average transfer functions from the adapter and the slip table to the sensory ring (fig. 2) in the octave-band random tests. The transfer function from the adapter to the sensory ring is measured in multimodal fixture test with small shaker excitation, and the transfer function from the slip table to the sensory ring is measured in the test in which the ring is mounted directly on the slip table. The data indicate that the transfer function from the slip table to the sensory ring is much higher than the transfer function from the adapter to the sensory ring. This result is expected, since the spacecraft significantly loads the lightweight adapter, whereas the spacecraft has little effect on the fixture vibration levels.

This data emphasizes the difficulty of relating flight measurements of vibration to conventional rigid fixture vibration test specifications. If one measures the space-average vibration level on the Nimbus adapter during flight and specifies the level on the Nimbus adapter in a vibration test, the test results will be realistic. However if one measures the space-average vibration level on the Nimbus adapter and then specifies the levels on a conventional test fixture attached to the spacecraft ring, the tests would result in disastrous overtesting. In order to specify and control vibration tests on the basis of space-average vibration levels on a reverberant structure, it is necessary to insure that the mounting fixture impedance simulates the impedance of the inflight mounting structure.

Figures 20, 21, and 22 present the space-average transfer functions from the spacecraft adapter to the sensory ring, control box, and solar panels (see fig. 2) for four different excitation configurations. In the first configuration the adapter is excited directly with three small shakers, in the second configuration the adapter is mounted on the multimodal fixture which is excited with three small shakers, in the third configuration the adapter is mounted directly on the slip table and excited with horizontal excitation, and in the fourth configuration the adapter is mounted on a multimodal fixture which is in turn mounted on a slip table and excited with horizontal excitation. The data in figs. 20, 21, and 22 indicate that the transfer function from the adapter to the spacecraft elements when the adapter is excited directly with small shakers is significantly less than the transfer function when the adapter is mounted on the multimodal fixture or conventional slip table. These data suggest that high-frequency

vibration tests utilizing small shakers to directly excite an element of the spacecraft structure may undertest other elements of the spacecraft.

The transfer functions from the adapter to the sensory ring and control box obtained with the adapter mounted on the multimodal fixture excited with small shakers are lower than the transfer functions obtained with the multimodal fixture excited by a slip table. The transfer functions from the adapter to the sensory ring, control box, and solar panels when the adapter is excited directly with slip table excitation and when the adapter is mounted on a multimodal fixture excited with slip table excitation are similar.

Effect of Excitation and Measurement Axes

Figure 23 shows the space-average transfer functions from the multimodal fixture to the adapter for different excitation axes in the octave-band random tests. In the first test the multimodal fixture is excited with three shakers acting along three radii of the multimodal fixture (fig. 4), in the second test the multimodal fixture is excited in the longitudinal direction with a conventional fixture, in the third test the multimodal fixture is excited along the x-horizontal axis of the slip table, and in the fourth test the multimodal fixture is excited along the y-horizontal axis of the slip table. The data presented in fig. 23 indicate that the transfer function from the fixture to the adapter in the small shaker excitation test generally corresponds with the transfer functions in the horizontal excitation slip table tests, whereas the transfer function in the longitudinal slip table test differs significantly from the horizontal excitation test results.

Figure 24 shows the transfer functions from the mount to the adapter for different mount excitation axes in octave-band random tests. In these tests the adapter response is measured in the axial, radial, and tangential direction at a single point and these measurements are averaged together to yield a measure of the axis-average adapter response. In the first test, the adapter is mounted on the multimodal fixture excited along the radial direction with three small shakers and the mount input measured with a horizontal accelerometer on the fixture, in the

second test the adapter is mounted on a conventional fixture excited in the longitudinal direction and the input is measured with a longitudinal accelerometer on the fixture, in the third test the adapter is mounted on a slip table excited in the x-horizontal axis and the input is measured with a x-axis accelerometer on the fixture, and in the fourth test the adapter is mounted on a slip table excited in the y-horizontal axis and the input is measured with a y-axis accelerometer on the fixture. The data in fig. 24 indicate that the measurement-axis-average transfer function obtained with the adapter mounted on the multimodal fixture excited in the radial direction envelopes the measurement-axis-average transfer functions obtained with the adapter mounted on the conventional fixture and on the slip table.

Figure 25 presents the spread of the response measurements in the radial, tangential, and axial direction on the spacecraft adapter in multimodal fixture tests with radial small shaker excitation and in the slip table test with x-horizontal axis excitation. The data indicate that the variation in the adapter response along the three axes is much less in the multimodal fixture excitation test than in a conventional slip table test. Thus the multimodal fixture configuration with small shaker excitation provides a response on the adapter which is more tri-axial than the conventional uniaxial slip table vibration test.

Maximum Acceleration Levels Obtainable

The disparity between the shaker size in the conventional-fixture configuration shown in fig. 1 and the shaker size in the multimodal fixture test configuration shown in fig. 2 leads to the question, "What are the maximum acceleration levels obtainable on the spacecraft with the multimodal fixture, small shaker configuration?" Figure 26 presents the maximum obtainable acceleration levels on the model spacecraft elements with the multimodal fixture mounting configuration excited with three small (25-lb force shakers). In octave-band random tests, the space-average levels on the adapter range from 2 to 20 g's rms in the various octave bands. In sine tests at the discrete frequencies of 20, 100, and 1000 Hz the maximum obtainable acceleration levels on the adapter are comparable with those in the octave band random tests. The maximum obtainable

levels on the sensory ring in the sine tests range from approximately 1 to 3 g's. The maximum obtainable acceleration levels on the control box and solar panels are approximately 1/2 g rms, at the high frequencies in the sine tests reflecting the attenuation through the spacecraft at the high frequencies.

The fact that it is possible to obtain 1 g rms acceleration levels on the spacecraft sensory ring at frequencies of 20, 100, and 1000 Hz indicates that in the high-frequency regime, the three small 25-lb force shakers are almost adequate for simulating high-frequency vibration environments produced by present-day space vehicles. In actual spacecraft test programs utilizing multimodal test fixtures, one would probably wish to use somewhat larger shakers than used here, however the disparity between the 25-lb force shakers used in our experiments and the 30,000-lb force shaker typically used in high-frequency vibration tests is startling. These test results presented herein indicate that the need for very high-force shakers for high-frequency vibration tests is associated with the peculiar methods of performing conventional tests rather than with requirements pertaining to the simulation of high-frequency vibration environments.

SUBSTITUTE ACOUSTIC TEST RESULTS

In the environmental checkout of aerospace structures, it is becoming common practice to require full-scale prototype acoustic tests. Recently acoustic testing techniques have been advocated as a method of overcoming problems associated with conventional vibration test fixture setups in the high-frequency regime (ref. 8). A series of experiments were conducted to determine the relative efficiencies of acoustical and mechanical excitations of the 1/2-scale model spacecraft and to determine the feasibility of utilizing small shakers attached directly to the spacecraft to simulate the response of the spacecraft to a reverberant acoustic field.

Efficiency of Acoustical and Mechanical Excitation

Instrumentation for measuring electrical power into an acoustic speaker or mechanical shaker and for measuring

the mechanical power transferred from the mechanical shaker to the multimodal test fixture is shown in fig. 27. In the first experiment, a large electrodynamic speaker (a JBL model S7 system) is placed approximately 2 ft. from the 1/16 in. multimodal test fixture and the fixture is excited with octave-bands of acoustic noise. The measured electrical power into the speaker to create a 1 "g" rms space-average acceleration level on the fixture in the octave bands are shown in fig. 28. (It was not possible to obtain 1 "g" levels on the fixture with the speaker available, so the speaker electrical power measurements shown in fig. 28 are scaled up from low-level test data.) In the second experiment, a 25-lb force shaker is attached directly to the fixture and the electrical power into the shaker required to produce a 1 "g" rms space-average response on the fixture is measured. The measured shaker electrical power in octave-bands is also shown in fig. 28. The results of these tests indicate that for 1 "g" acceleration level on the fixture, the electrical power required to drive the exciting speaker would be approximately 1000 times as large as the electrical power required to drive a shaker attached directly to the fixture.

In the second experiment, the mechanical power transferred from the shaker to the fixture is measured using the impedance head shown in fig. 27, and this data is also plotted in fig. 28. The shaker is approximately 30% efficient at 125 cycles and approximately 1% efficient at 1000 Hz. To confirm the measurements of mechanical power into the fixture, the power dissipated internally in the fixture, and the power transferred from the fixture to the model spacecraft is calculated for the case of 1 "g" rms space-average fixture response.

The time-average power dissipated in the fixture is calculated from Eq. 5.

$$P_1 = \frac{\eta M \langle a_1^2 \rangle_{s,t}}{2\pi f} \quad (5)$$

where η is the damping loss factor of the fixture given by fig. 9, M is the fixture mass. and $\langle a^2 \rangle_{s,t}$ is the space-average acceleration level of the fixture (ref. 9).

The time-average power transferred from the fixture to the spacecraft is calculated using the statistical energy analysis relation given by eq. 6

$$P_{12} = \frac{\eta_{12}}{2\pi f} [M_1 \langle a_1^2 \rangle_{s,t} - M_2 \frac{\delta_2}{\delta_1} \langle a_2^2 \rangle_{s,t}] \quad (6)$$

where M_1 is the mass of the fixture, M_2 is the mass of the spacecraft adapter, δ_2 is the modal separation of the spacecraft adapter, δ_1 is the modal separation of the multimodal fixture, $\langle a_1^2 \rangle_{s,t}$ is the space-average acceleration of the multimodal fixture, $\langle a_2^2 \rangle_{s,t}$ is the space-average acceleration of the spacecraft adapter, and η_{12} is the coupling loss factor from the fixture to the adapter (eq. 12 of ref. 9). The coupling loss factor η_{12} is calculated by modifying results for two coupled plates (eq. 36 of ref. 4) to account for the effect of curvature on the speed of bending waves in the multimodal fixture. The calculated power dissipated in the fixture and the power transferred to the spacecraft are also shown in fig. 29. The sum of the power dissipated in the fixture and the power transferred from the fixture to the spacecraft is approximately equal to the measured mechanical power into the fixture from the shaker and therefore the power balance measurements are confirmed. These calculations also indicate that the power dissipated in the fixture is approximately equal to the power transferred to the spacecraft, so the 1/16 in. multimodal fixture is approximately 50% efficient.

Acoustic and Mechanical Excitation of Model Spacecraft

In the first series of tests the model Nimbus spacecraft is excited with a reverberant sound field with octave-bands of random noise, and the resulting space-average acceleration responses of the adapter, solar panels, and control box are shown by the solid lines in fig. 29. The adapter and solar panels appear to be the most important receivers of acoustic power.

In the second experiment, one small shaker is attached to the spacecraft adapter and a second shaker is attached to the spacecraft solar panels. The excitation levels for these two shakers are adjusted so as to simulate the calculated response of the adapter and solar panels to acoustic excitation. The acceleration response of the adapter, solar panels, and the spacecraft control box in the mechanical excitation experiment are also shown in fig. 29.

The results indicate that even though the acoustic response of the adapter and solar panels are adequately simulated in the mechanical excitation experiment, the spacecraft control box levels are significantly less in the mechanical excitation experiment than in the acoustic excitation experiment. These results indicate that it is not feasible to utilize local mechanical excitation from two small shakers to simulate the response of the complete model Nimbus spacecraft to a reverberant acoustic field.

CONCLUSIONS AND RECOMMENDATIONS

The test data obtained in this investigation supports the following conclusions:

- 1) It is possible to construct small multimodal vibration test fixtures to simulate the average point impedance and modal density of large aerospace mounting structures in the high-frequency regime. The multimodal fixture designed in this investigation results in apparently realistic transfer functions, relatively smooth frequency response, and small spatial variations at frequencies above approximately 50 Hz. This frequency is well below the frequencies at which the conventional fixture and slip table configurations begin to exhibit fixture resonance and unrealistic overtesting problems.
- 2) If the multimodal test fixture concept is employed, shakers, significantly smaller than those currently used in high-frequency vibration spacecraft tests are capable of exciting inflight vibration levels on the spacecraft. If a multimodal fixture or

simulated mounting structure is mounted on a conventional fixture and large shaker configuration, the fixture resonances will exhibit themselves through the multimodal fixture or mounting structure and adversely effect the test results.

- 3) If the multimodal fixture testing concept is employed, a single test can be conducted at high frequencies and the vibration environment on the spacecraft will simultaneously simulate the environment generated in conventional tests conducted along each of three perpendicular axes. Vibration tests utilizing the multimodal test fixture concept will generally result in a more triaxial spacecraft vibration environment in the high-frequency regime than tests performed with conventional fixtures excited along a single axis.
- 4) Acoustic excitation is a much less efficient method of exciting structures than mechanical excitation, but the response of a complex aerospace structure such as a spacecraft to distributed acoustic excitation cannot, in general, be simulated by attaching shakers directly to the spacecraft.

On the basis of the results of the present investigation, it is appropriate to recommend that:

- 1) Increased emphasis be placed on inflight vibration measurements on reverberant structures far removed from mounting point interfaces. Vibration measurements made on reverberant structures such as the space vehicle skin or a spacecraft adapter are in general more reliable and subject to less variation from flight to flight and less variation when the details of the mounting configuration or spacecraft are changed slightly. Measurements on reverberant structure also indicate less frequency variation and less variation from point-to-point than measurements at complex attachment points.
- 2) The multimodal fixture and small shaker test configuration be used in the high-frequency regime in future spacecraft test programs in order to eliminate the rather artificial problems associated with the use of conventional fixture and large shaker configurations.

- 3) Further research be conducted to determine the effect of mounting point impedance and vibration correlation along mounting-interfaces on the power transferred across the interface. It is well known that the power transferred between two structures connected at an interface depends not only on the average vibration level at the interface, but on the correlation of the vibration level at different points along the interface. Thus a rigid fixture which moves coherently will transmit more power to a test structure than a lightweight aerospace mounting structure which exhibits incoherent vibration, even though the space-average vibration levels at the interface are the same on the rigid fixture and the flexible mounting structure.
- 4) The feasibility of utilizing the multimodal fixture concept for simulating high-frequency pyrotechnic shock environments should be investigated. Many of the problems associated with current practices in high-frequency vibration tests are also present in current practices in high-frequency shock tests. A multimodal fixture, excited by any convenient means should provide a realistic approach to the simulation of high-frequency shocks such as those associated with pyrotechnic devices in aerospace vehicles.
- 5) The possibility of using mechanical shakers to simulate the response of aerospace structures to acoustic excitation should be explored further. The results of this investigation point out the inefficiencies of acoustic excitation as a means of exciting aerospace structures, but indicate the difficulty in using mechanical shakers to simulate the response of complex aerospace structures such as spacecraft to distributed acoustic fields. These results do not, however, preclude the possibility of using small shakers to simulate the acoustic response of uniform aerospace structures such as the launch vehicle skin or the shroud of a spacecraft.

REFERENCES

1. T. D. Scharton and T. M. Yang, "Development of Improved Vibration Tests of Spacecraft Assemblies", Bolt Beranek and Newman Inc. Report No. 1702, submitted to the Jet Propulsion Laboratory, California Institute of Technology, Pasadena, California 91103, under Contract No. 951990.
2. D. U. Noiseux and E. B. Meyer, "Application of Impedance Theory and Measurements to Structural Vibration", Technical Report AFFDL-TR-67-182, Wright-Patterson Air Force Base, Ohio, 45433, January 1968.
3. E. E. Ungar and T. D. Scharton, "Analysis of Vibration Distribution in Complex Structures", Shock and Vibration Bulletin, 36, Part V, January 1967.
4. R. H. Lyon and E. Eichler, "Random Vibration of Connected Structures", Journal of the Acoustical Society of America, 36 (7), 1344, 1964, Equation 13.
5. R. H. Lyon, "Statistical Analysis of Power Injection and Response in Structures and Rooms", Bolt Beranek and Newman Inc. Report No. TIR-65, 14 June 1967, Equation 69.
6. T. D. Scharton and T. M. Yang, "Statistical Energy Analysis of Vibration Transmission into an Instrument Package", Paper No. 67057, presented at the SAE National Aeronautics and Space Engineering and Manufacturing Meeting, Los Angeles, October 1967.
7. H. D. Carden and R. H. Hen, "A Study of the Effectiveness of Various Methods of Vibration Reduction on Simplified Scale Models of the Nimbus Spacecraft", NASA TN D-2418, August 1964, page 6.
8. R. W. Peverly, "Acoustically-Induced Vibration Testing of Spacecraft Components", Shock and Vibration Bulletin, 36, Part III, 1967.
9. J. E. Manning, R. H. Lyon and T. D. Scharton, "The Transmission of Sound and Vibration to a Shroud-Enclosed Spacecraft", Bolt Beranek and Newman Inc. Report 1431, submitted to NASA, Goddard Space Flight Center, Greenbelt, Maryland, October 1966, Equation 11.

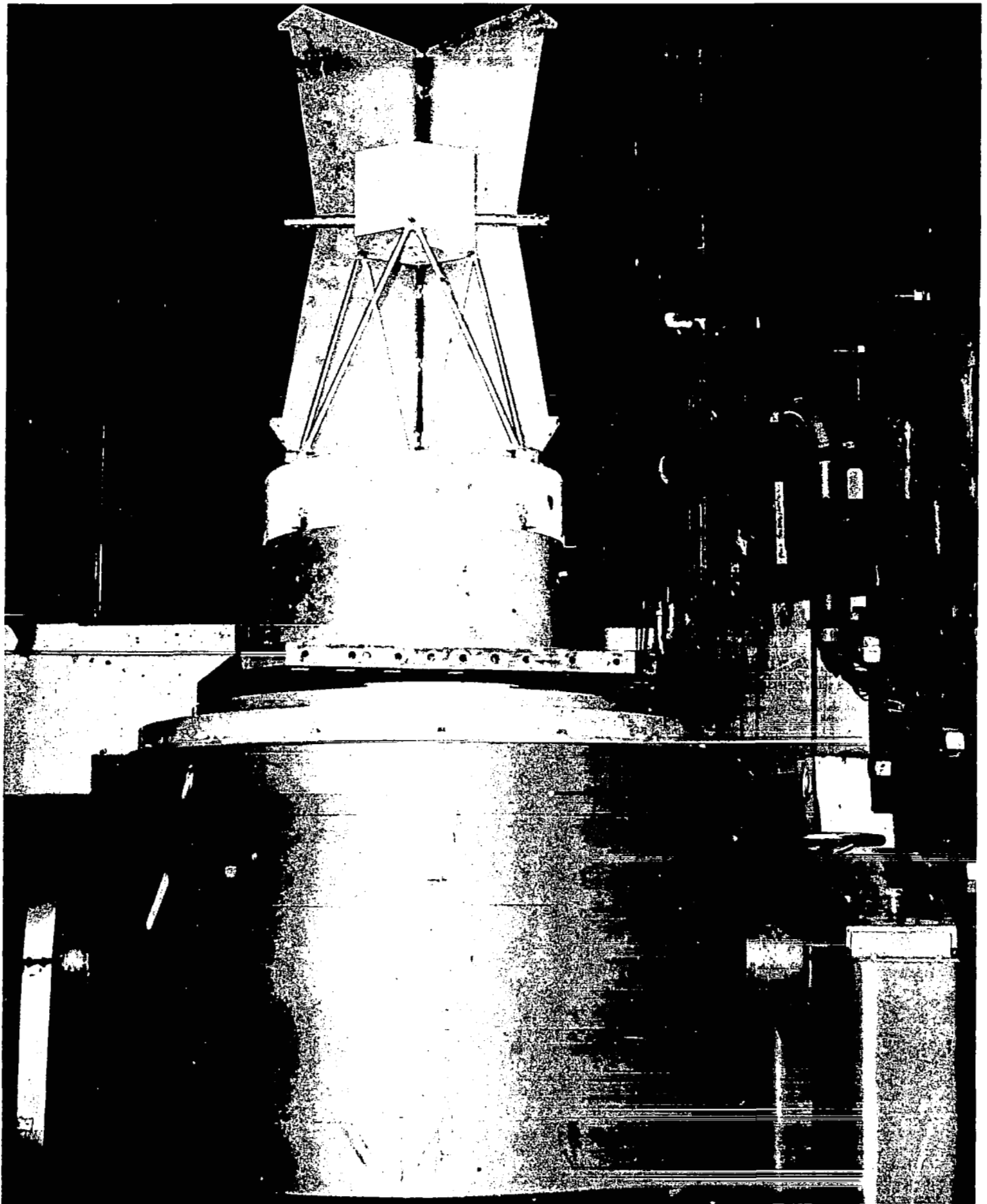


FIGURE 1. MODEL NIMBUS SPACECRAFT MOUNTED ON CONVENTIONAL
FIXTURE AND LARGE SHAKER CONFIGURATION

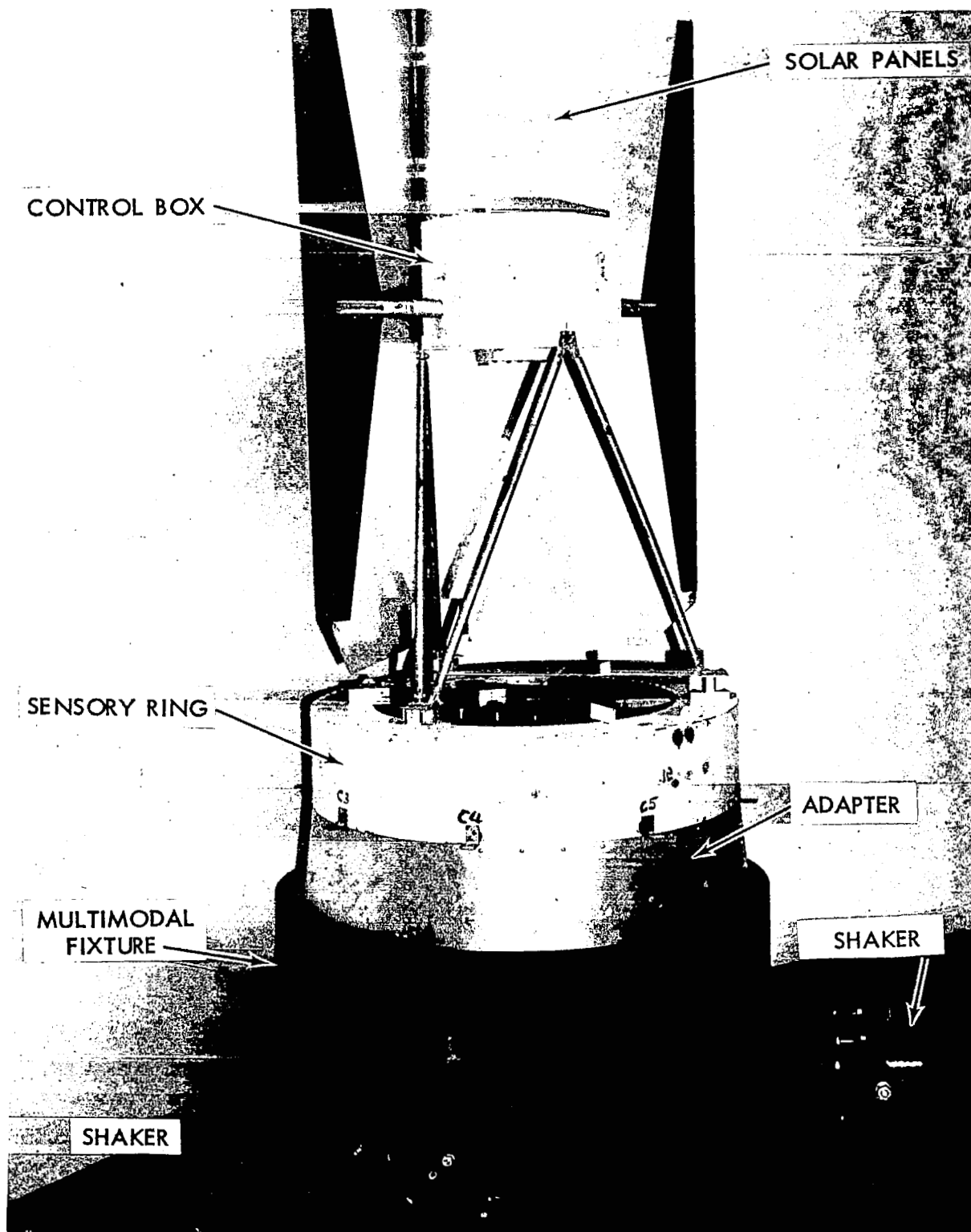


FIGURE 2. MODEL NIMBUS SPACECRAFT MOUNTED ON MULTIMODAL FIXTURE AND SMALL SHAKER CONFIGURATION

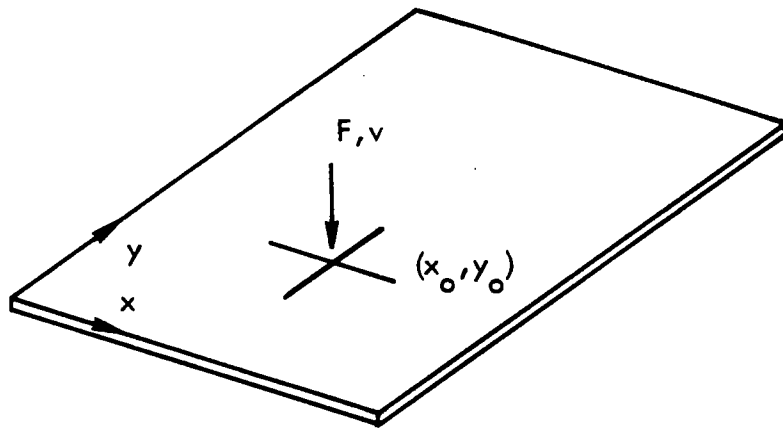


FIGURE 3A. PLATE IMPEDANCE MEASUREMENT SET-UP

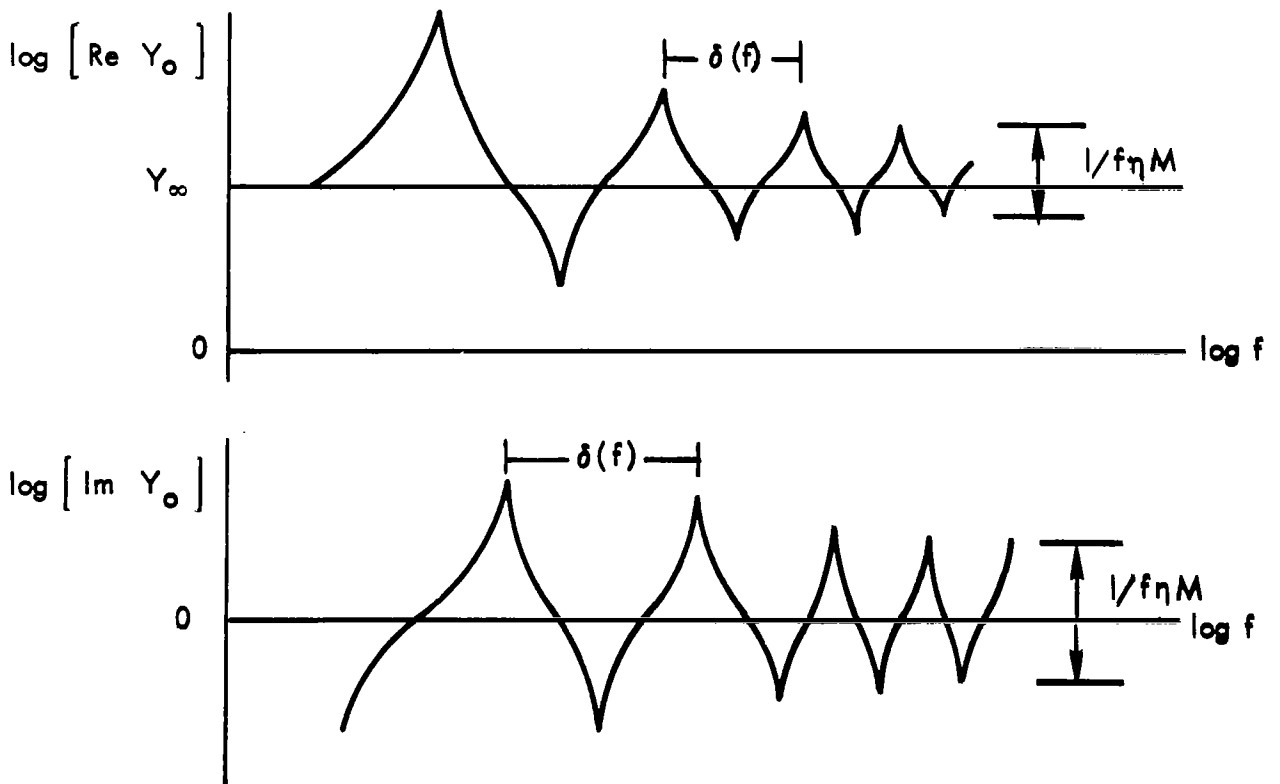


FIGURE 3B. TYPICAL PLATE IMPEDANCE DATA

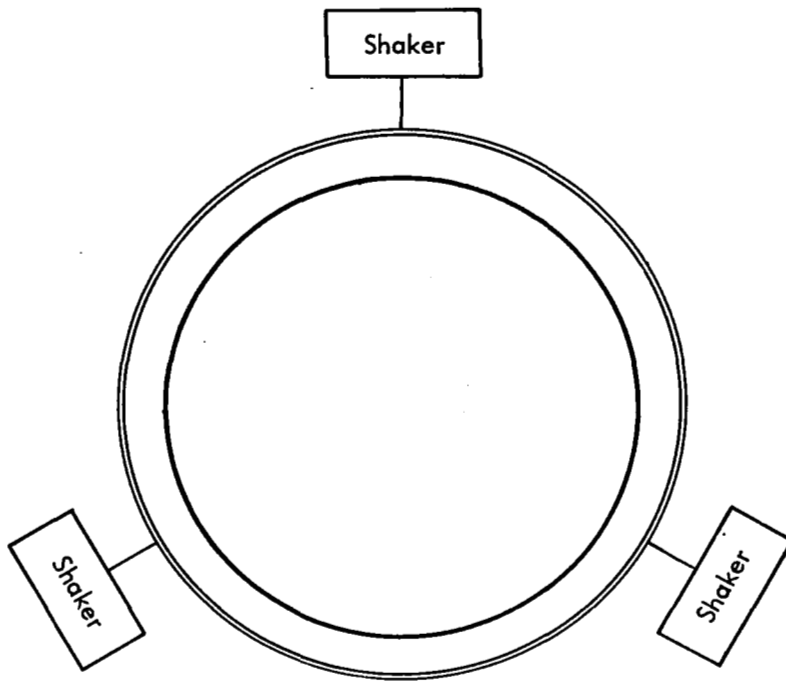


FIGURE 4A . TOP VIEW OF 1/16" CYLINDER AND SHAKER MOUNTING

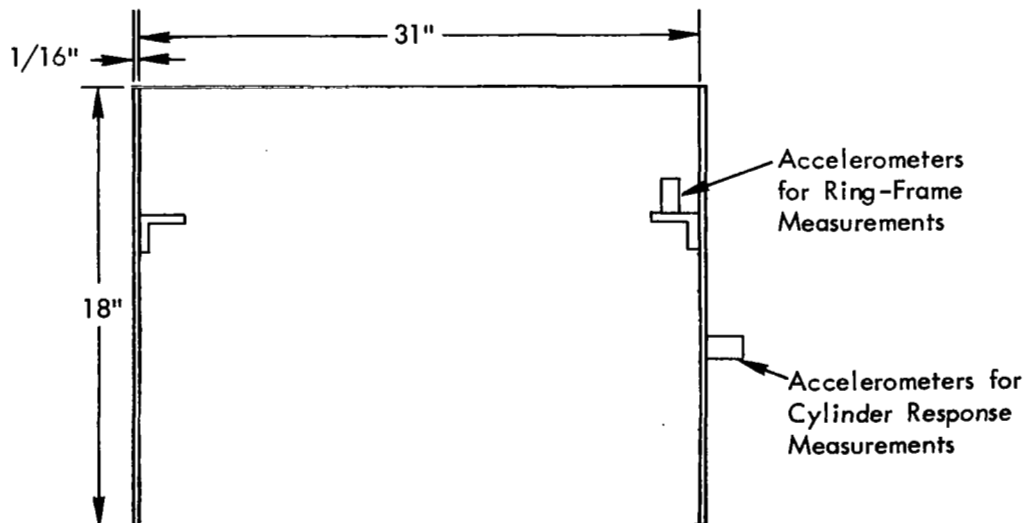


FIGURE 4B. CROSS-SECTION OF 1/16" CYLINDER

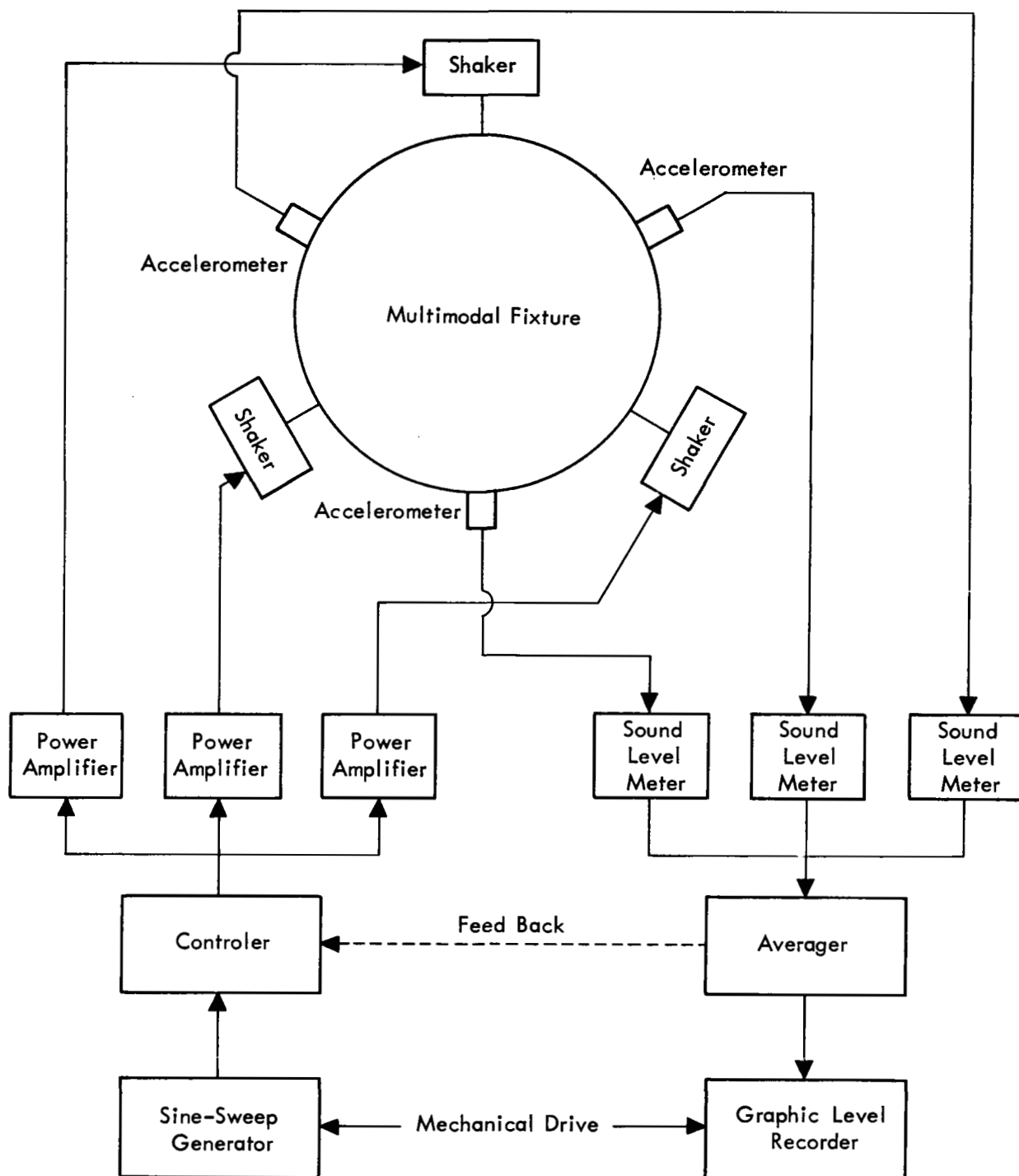


FIGURE 5. SINE-SWEEP TEST INSTRUMENTATION

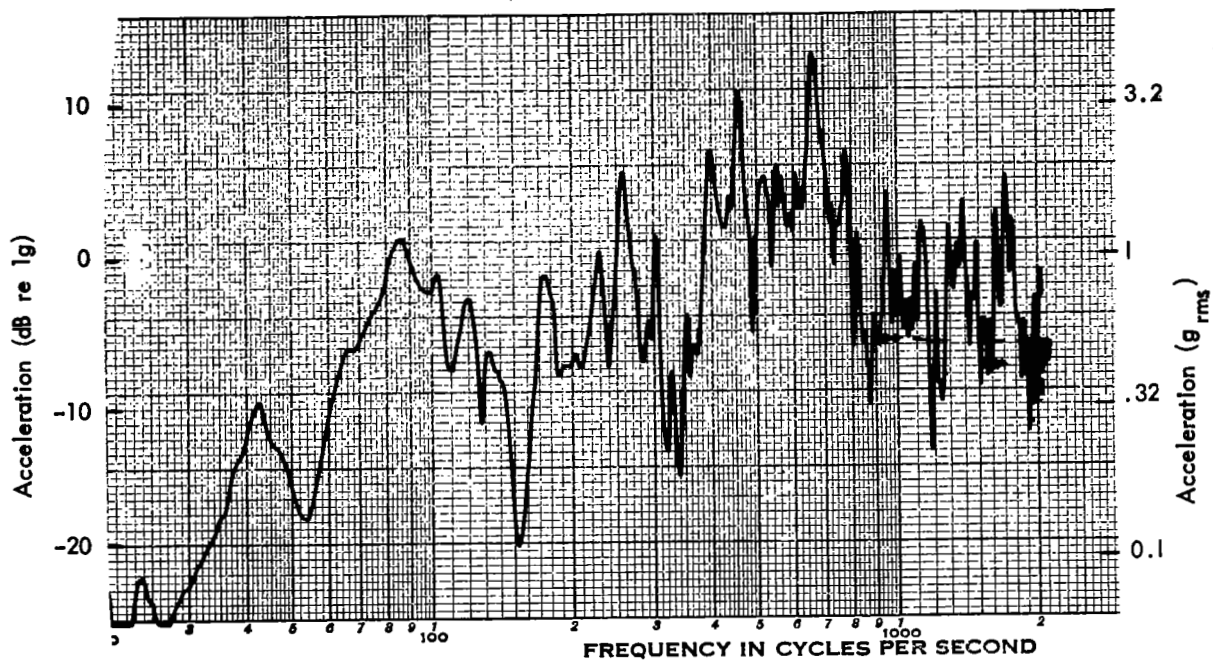


FIGURE 6A. SINE-SWEEP HORIZONTAL RESPONSE OF WALL OF 1/16" CYLINDER

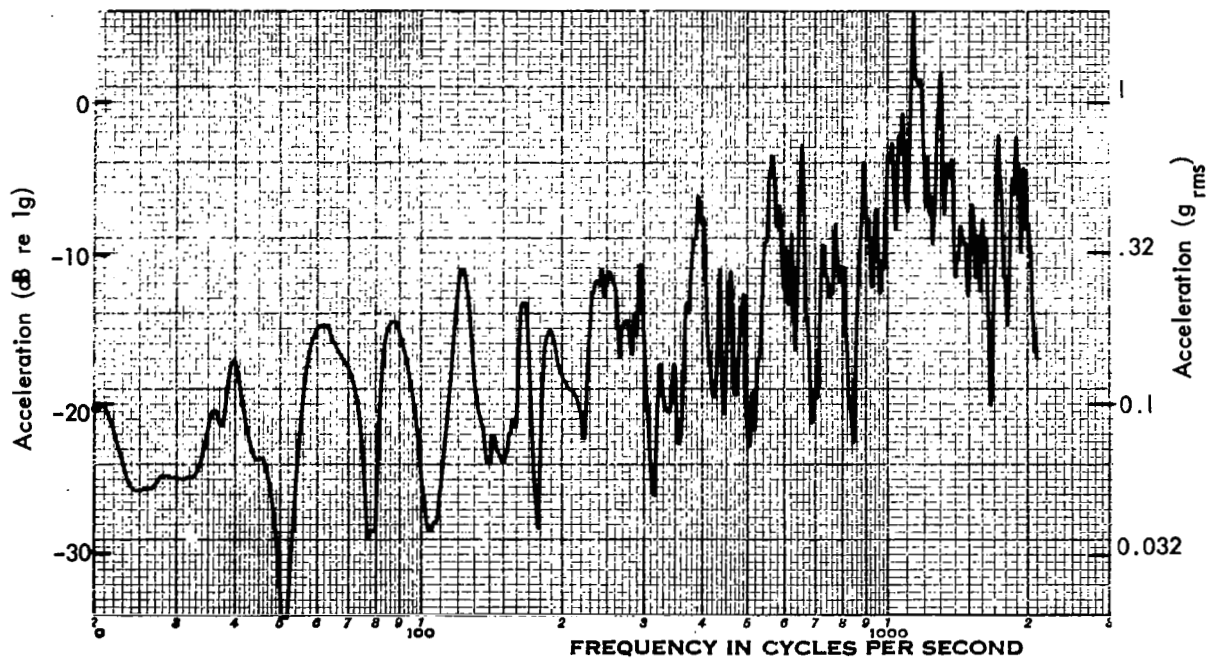


FIGURE 6B. SINE-SWEEP VERTICAL RESPONSE OF RING FRAME OF 1/16" CYLINDER

18 Horizontal Coils of Wire-Mesh Spaced
Uniformly Around Ring-Frame

Ring-Frame
Accelerometer

3 Wire-Mesh Plates

Ring-Frame

Cylinder
Accelerometer

Cylinder Wall

18 Vertical Coils of Wire-Mesh Spaced Uniformly
Around Cylinder Walls

FIGURE 7. CROSS-SECTION OF ENRICHED 1/16" CYLINDER

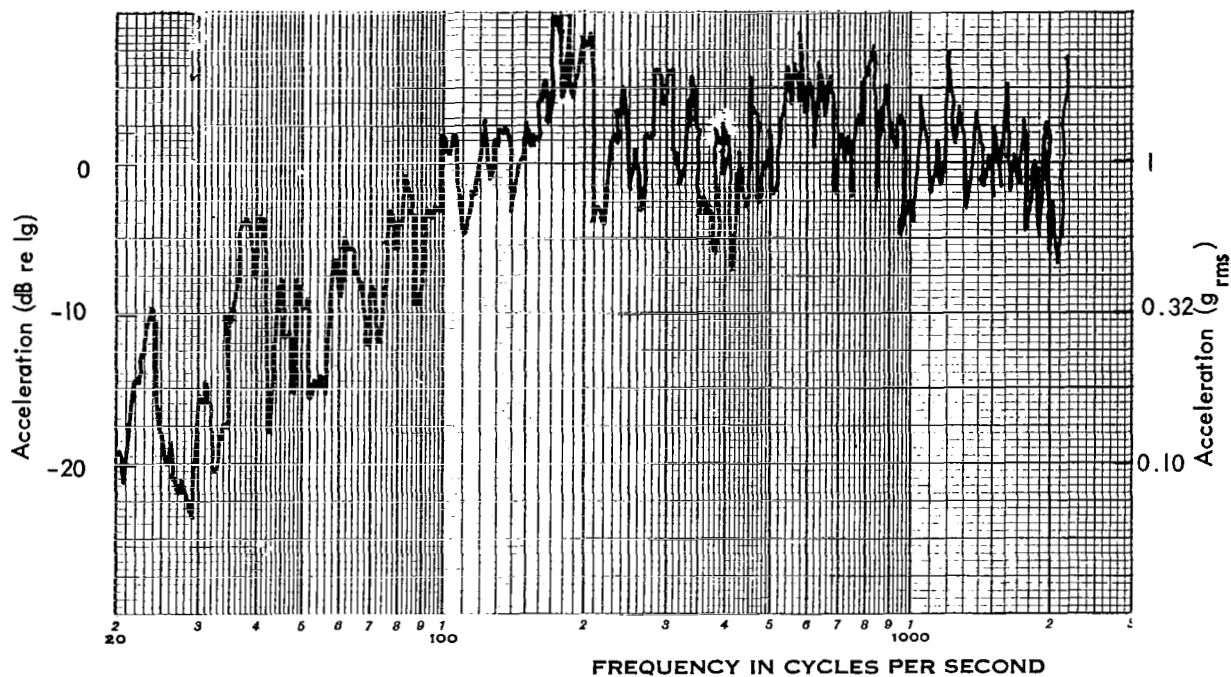


FIGURE 8A. SINE-SWEEP HORIZONTAL RESPONSE OF WALL OF ENRICHED 1/16" CYLINDER

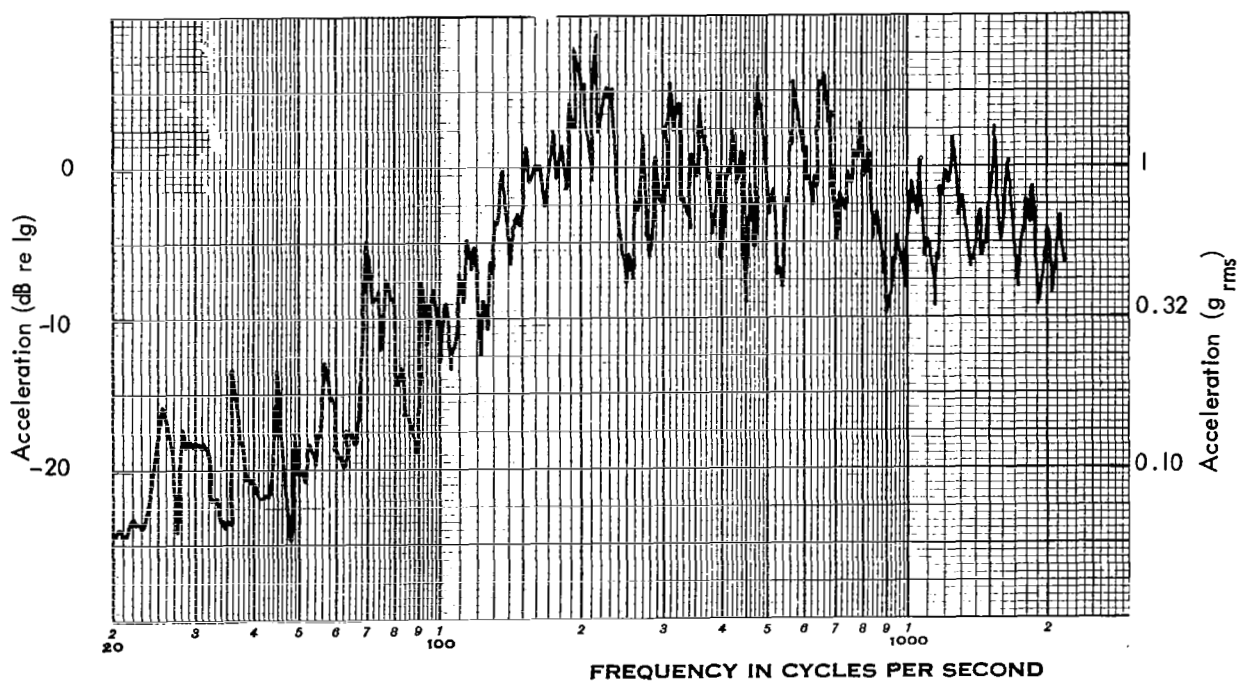


FIGURE 8B. SINE-SWEEP VERTICAL RESPONSE OF RING FRAME OF ENRICHED 1/16" CYLINDER

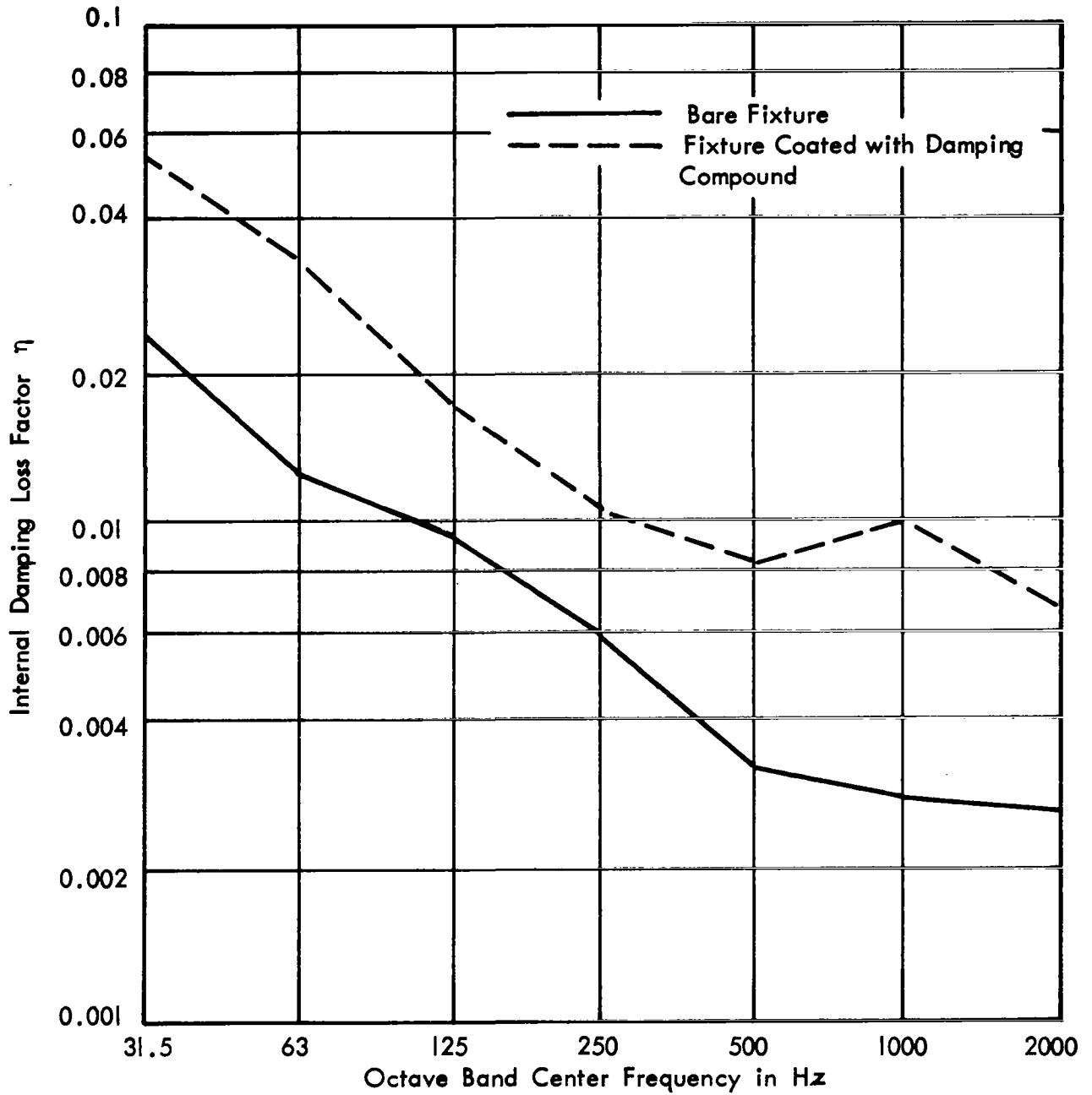


FIGURE 9. DAMPING OF 1/16" ENRICHED CYLINDER

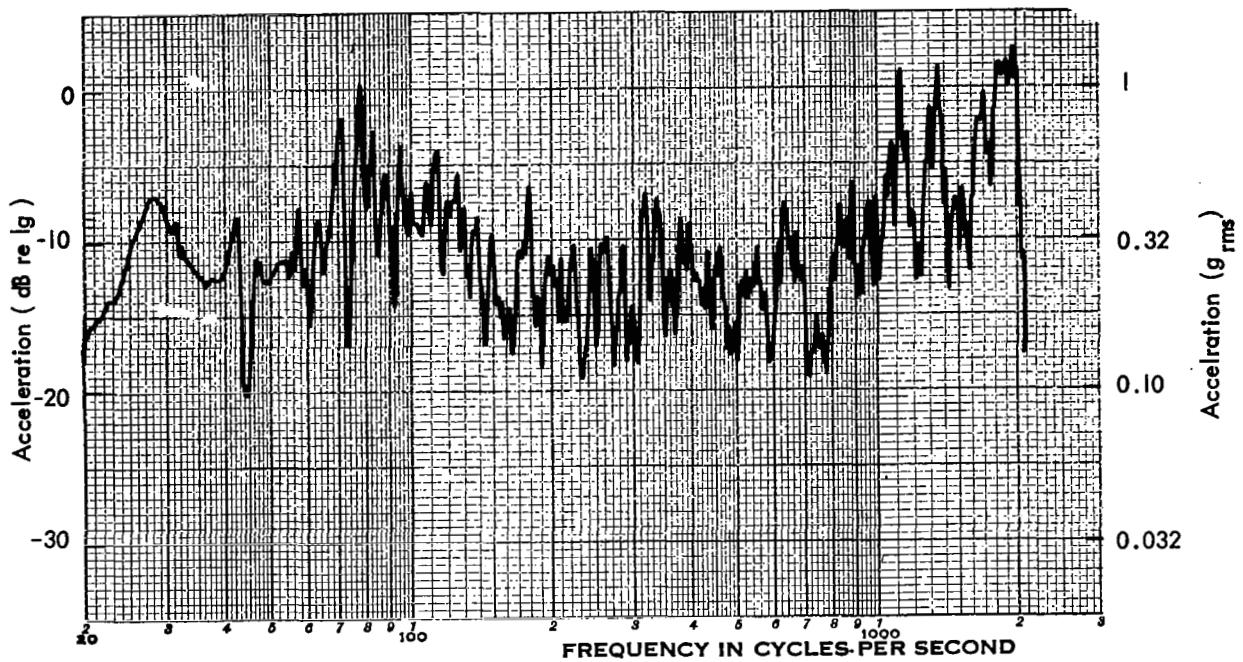


FIGURE 10A. SINE-SWEEP HORIZONTAL RESPONSE OF WALL OF ENRICHED, DAMPED 1/16" CYLINDER

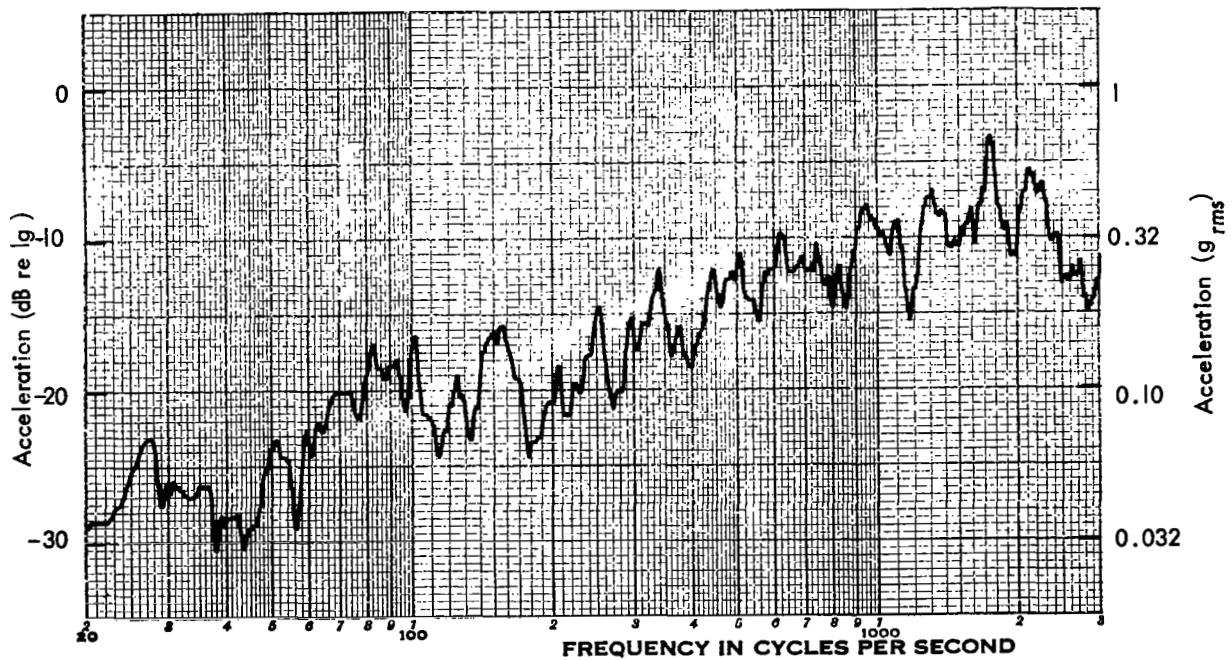


FIGURE 10B. SINE-SWEEP VERTICAL RESPONSE OF RING FRAME OF ENRICHED DAMPED 1/16" CYLINDER

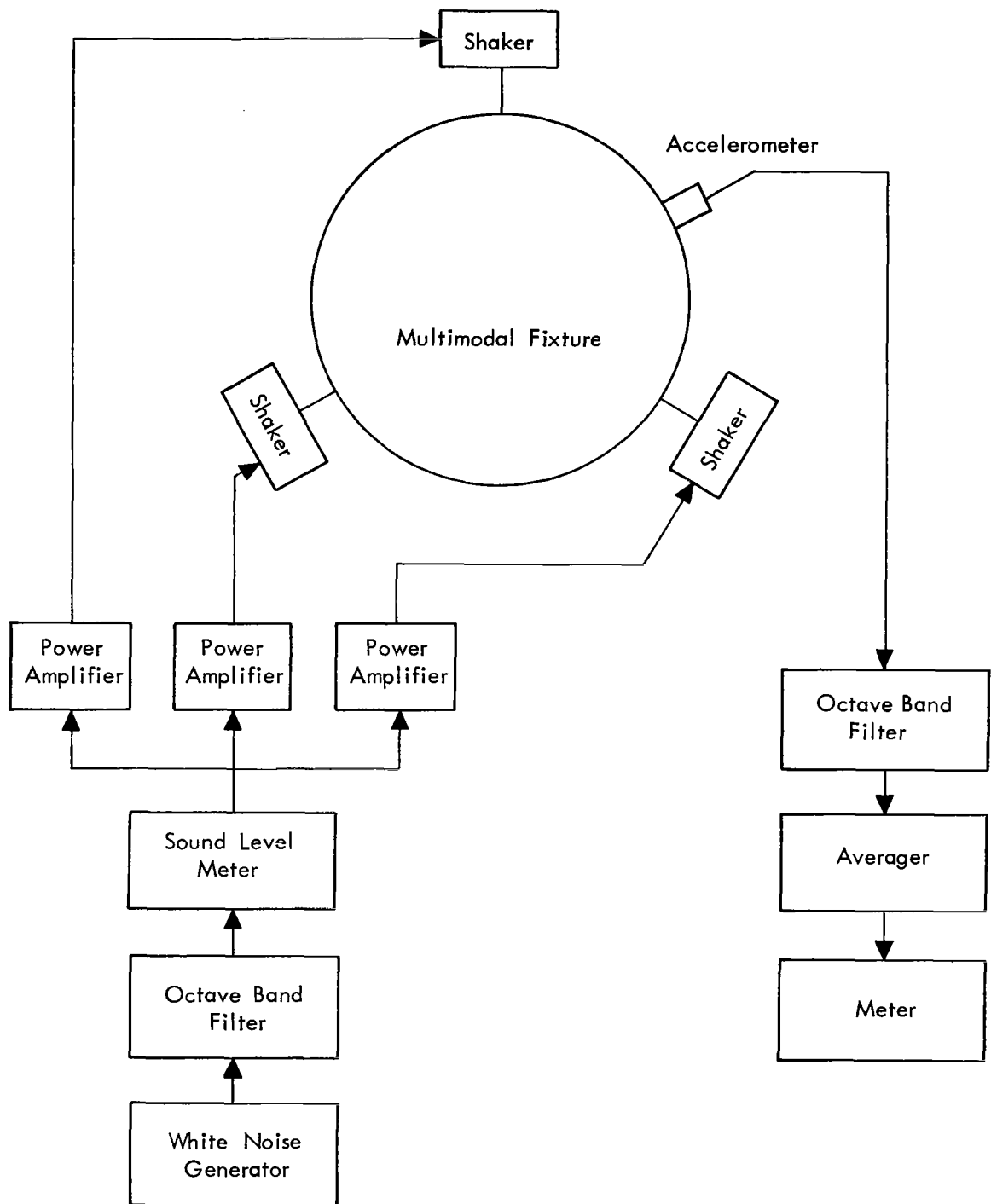


FIGURE II. OCTAVE-BAND RANDOM TEST INSTRUMENTATION

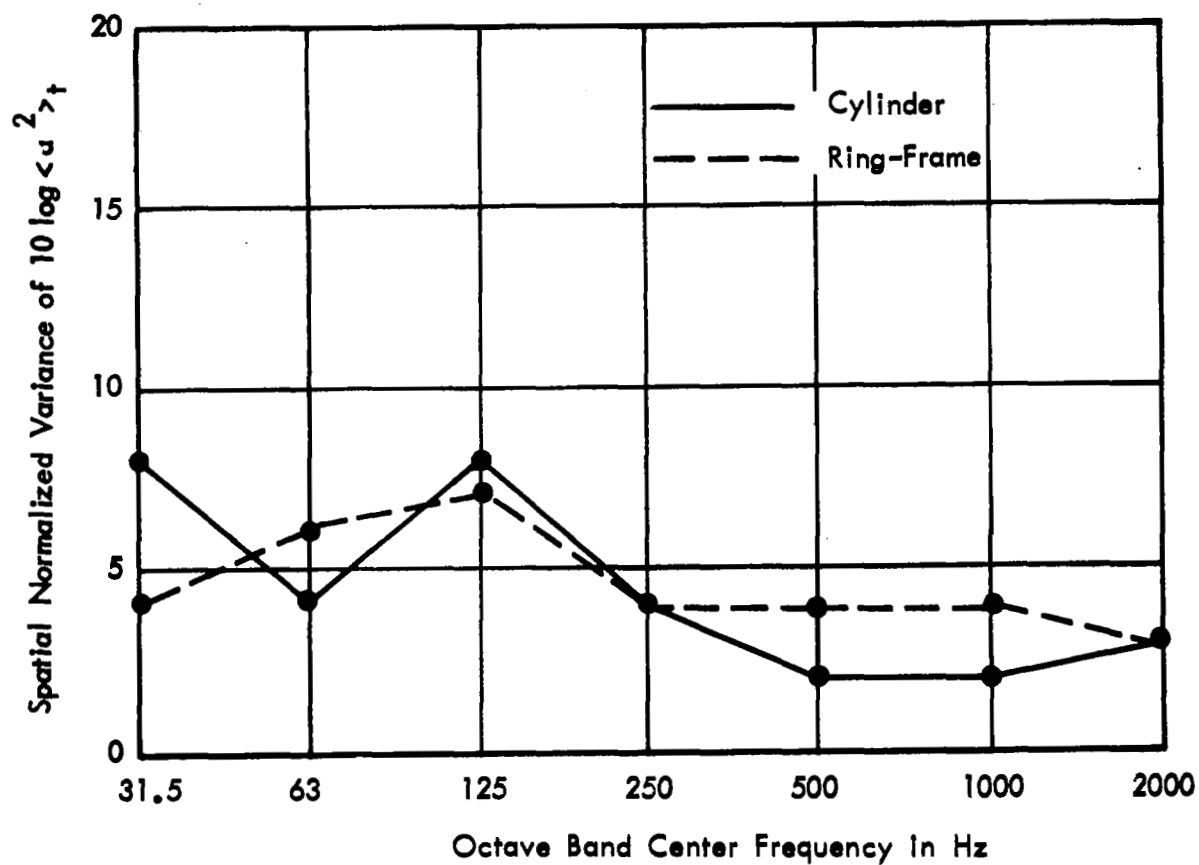


FIGURE 12. SPATIAL VARIATIONS OF ENRICHED DAMPED 1/16" CYLINDER

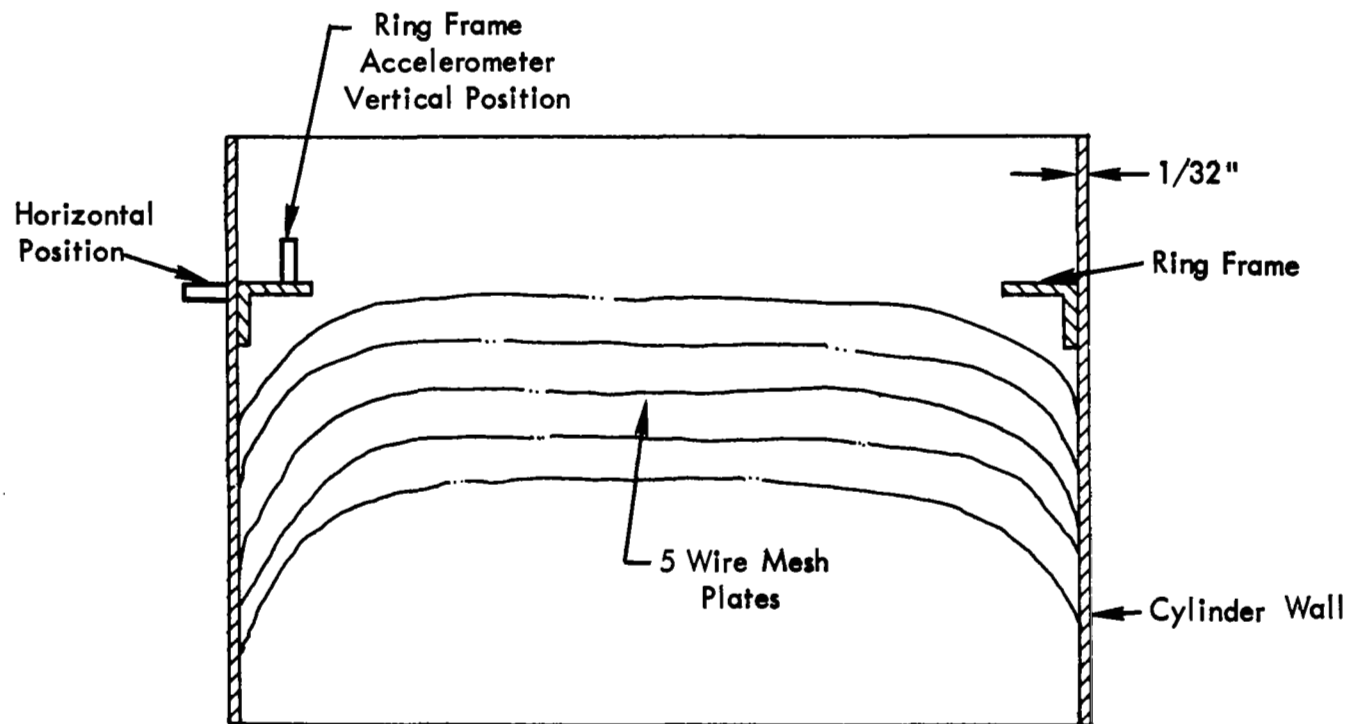


FIGURE 13. CROSS SECTION OF ENRICHED $1/32''$ CYLINDER

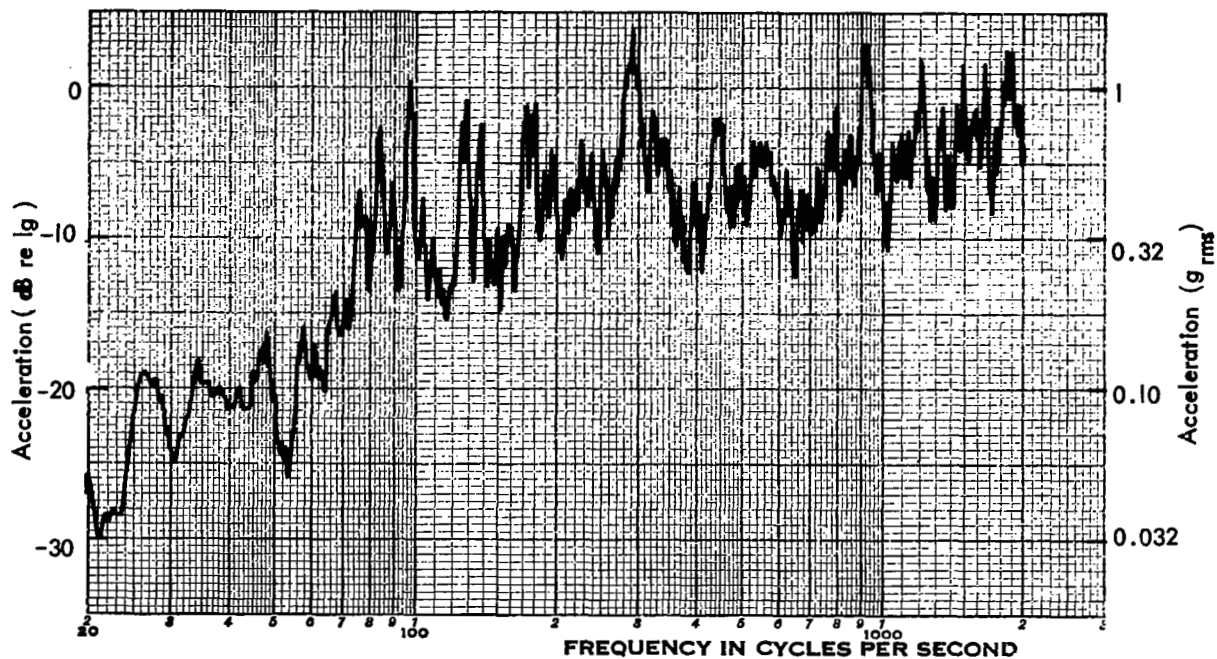


FIGURE 14A. SINE-SWEEP HORIZONTAL RESPONSE OF WALL OF ENRICHED 1/32" CYLINDER

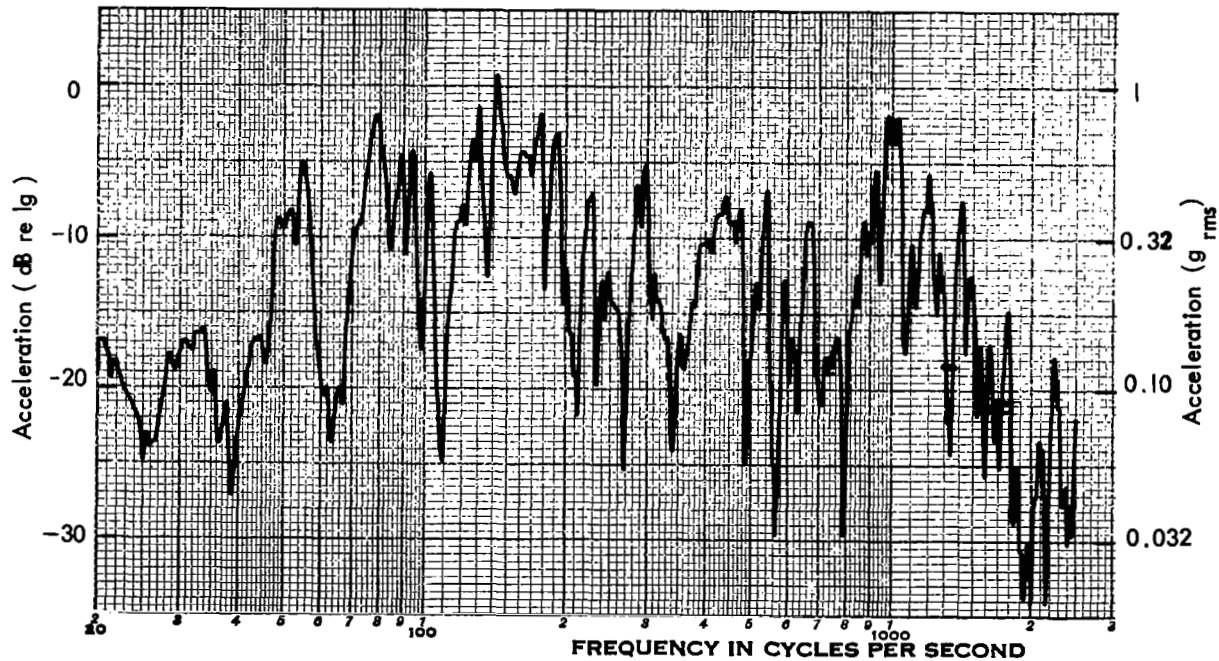


FIGURE 14B. SINE-SWEEP HORIZONTAL RESPONSE OF WALL OF ENRICHED AND DAMPED 1/32" CYLINDER

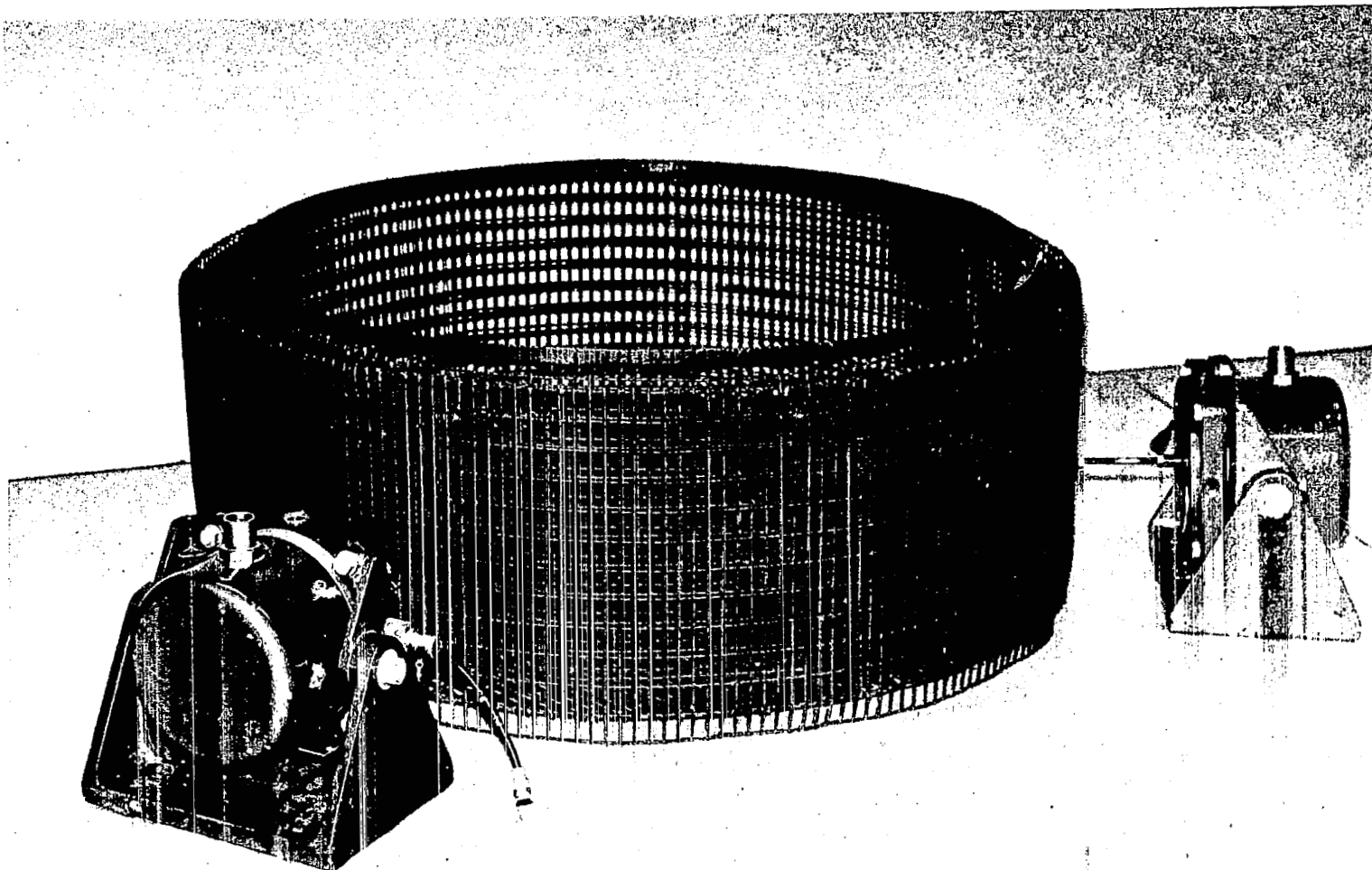


FIGURE 15. WIRE-MESH FIXTURE

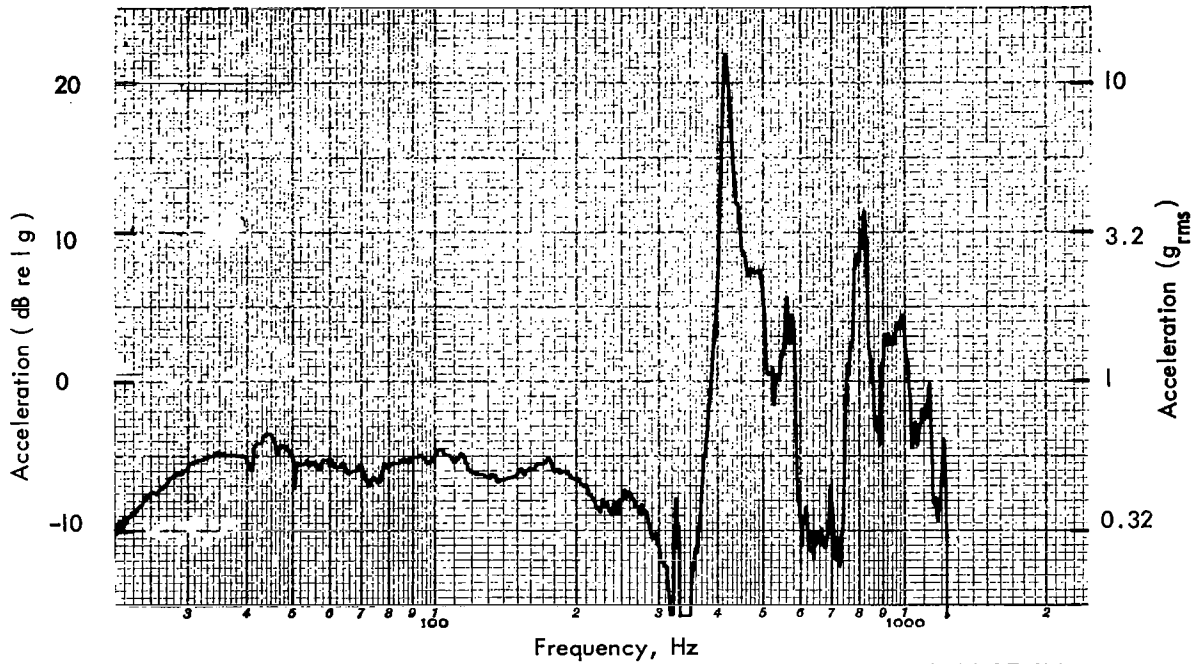


FIGURE 16A. SINE-SWEEP RESPONSE OF MULTIMODAL FIXTURE FOOT IN LONGITUDINAL CONVENTIONAL FIXTURE TEST

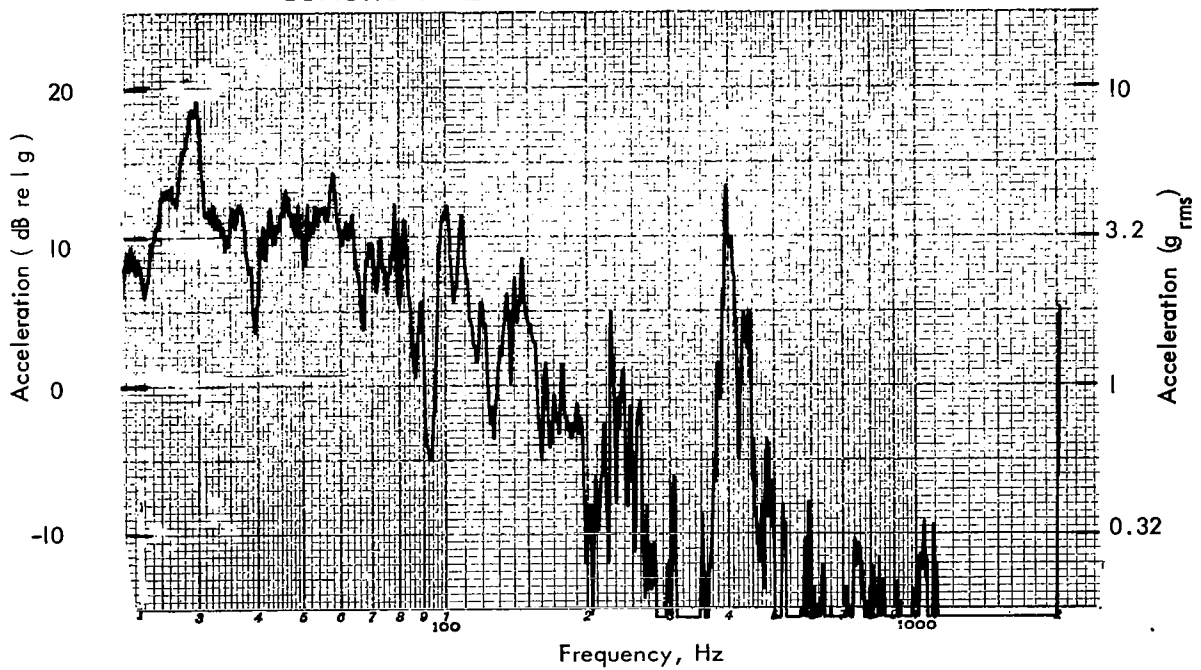
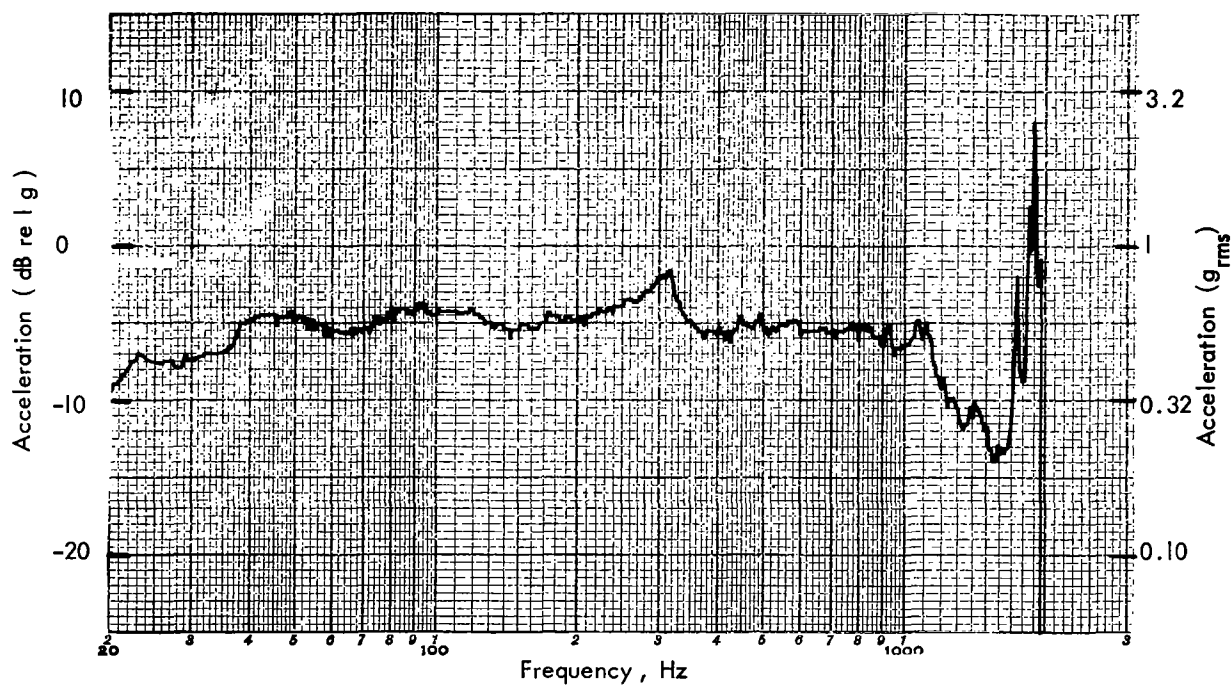
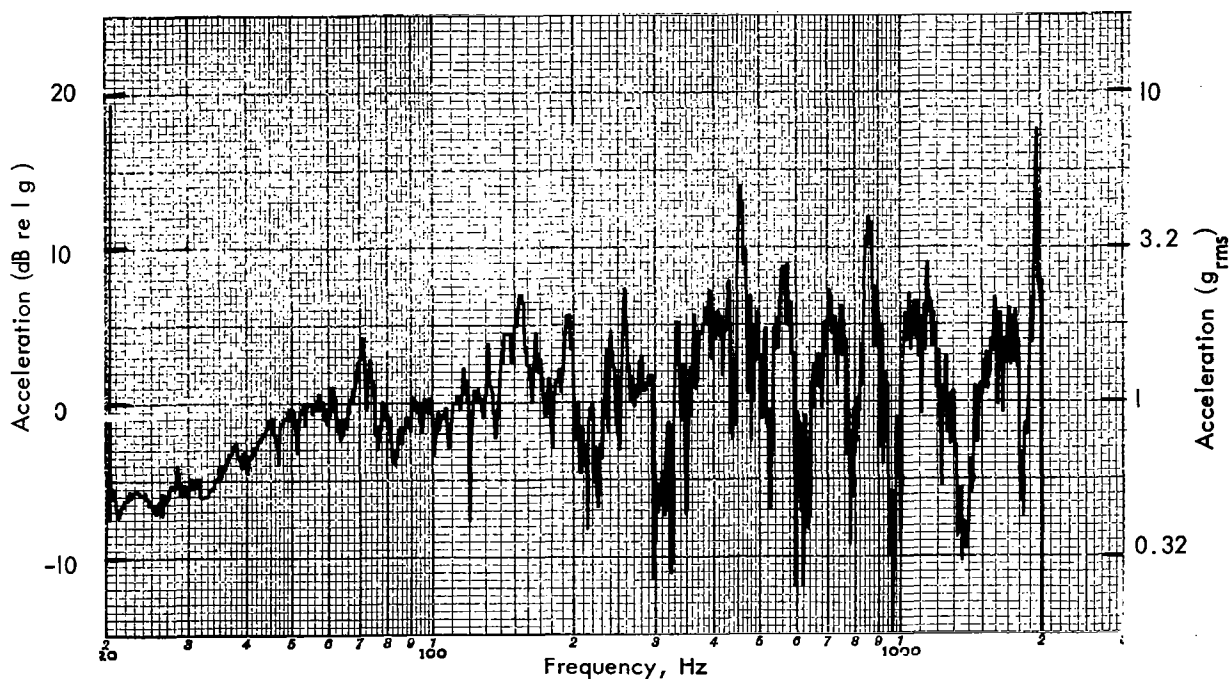


FIGURE 16B. SINE-SWEEP RESPONSE OF SOLAR PANEL IN LONGITUDINAL CONVENTIONAL FIXTURE TEST



FIXTURE 17A. SINE-SWEEP CONTROL RESPONSE OF SLIP TABLE IN HORIZONTAL CONVENTIONAL FIXTURE TEST



FIXTURE 17B. SINE-SWEEP RESPONSE OF MULTIMODAL FIXTURE IN HORIZONTAL CONVENTIONAL FIXTURE TEST

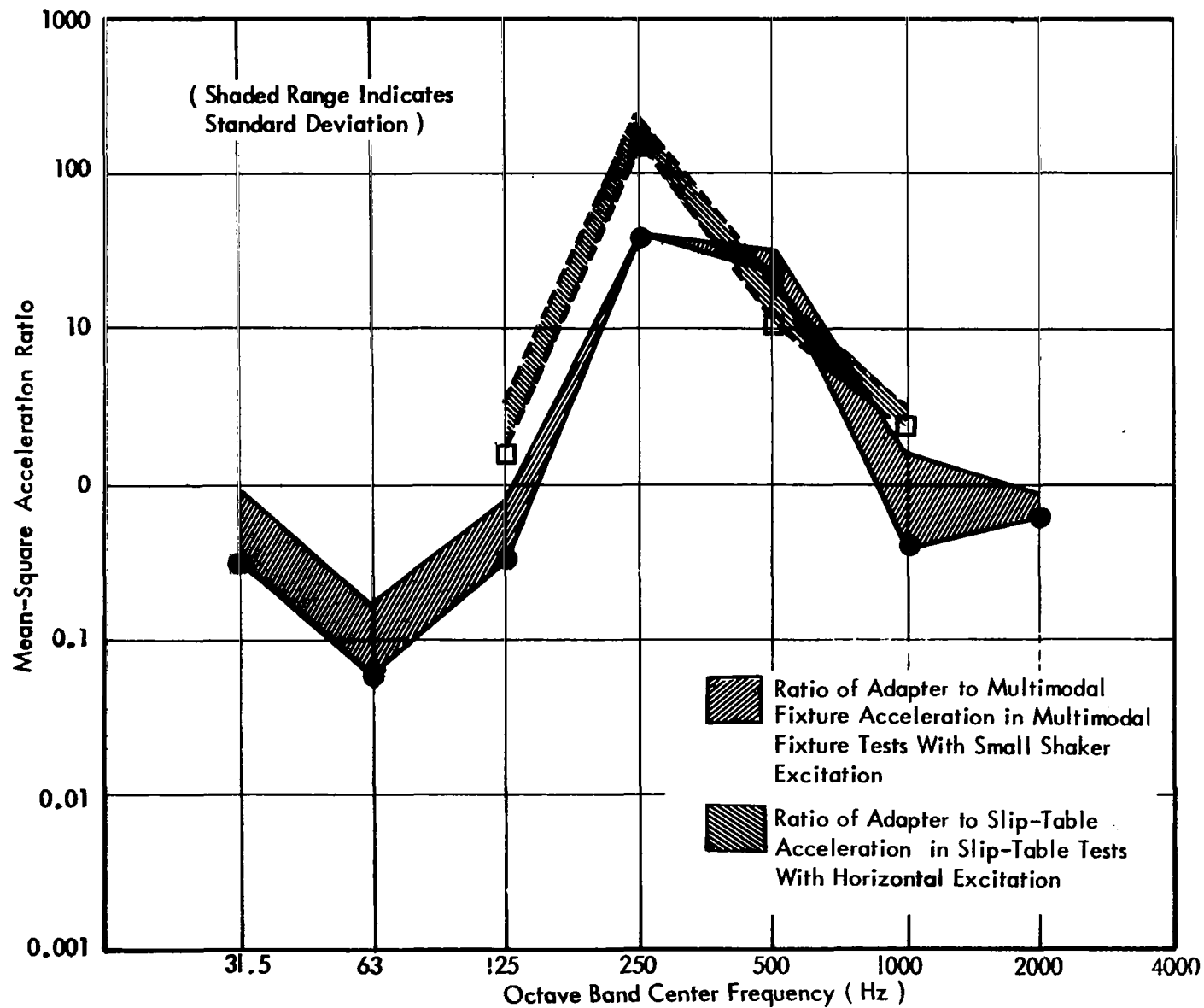


FIGURE 18. AVERAGE TRANSFER FUNCTIONS FROM MULTIMODAL FIXTURE AND SLIP - TABLE TO ADAPTER IN OCTAVE BAND RANDOM TESTS

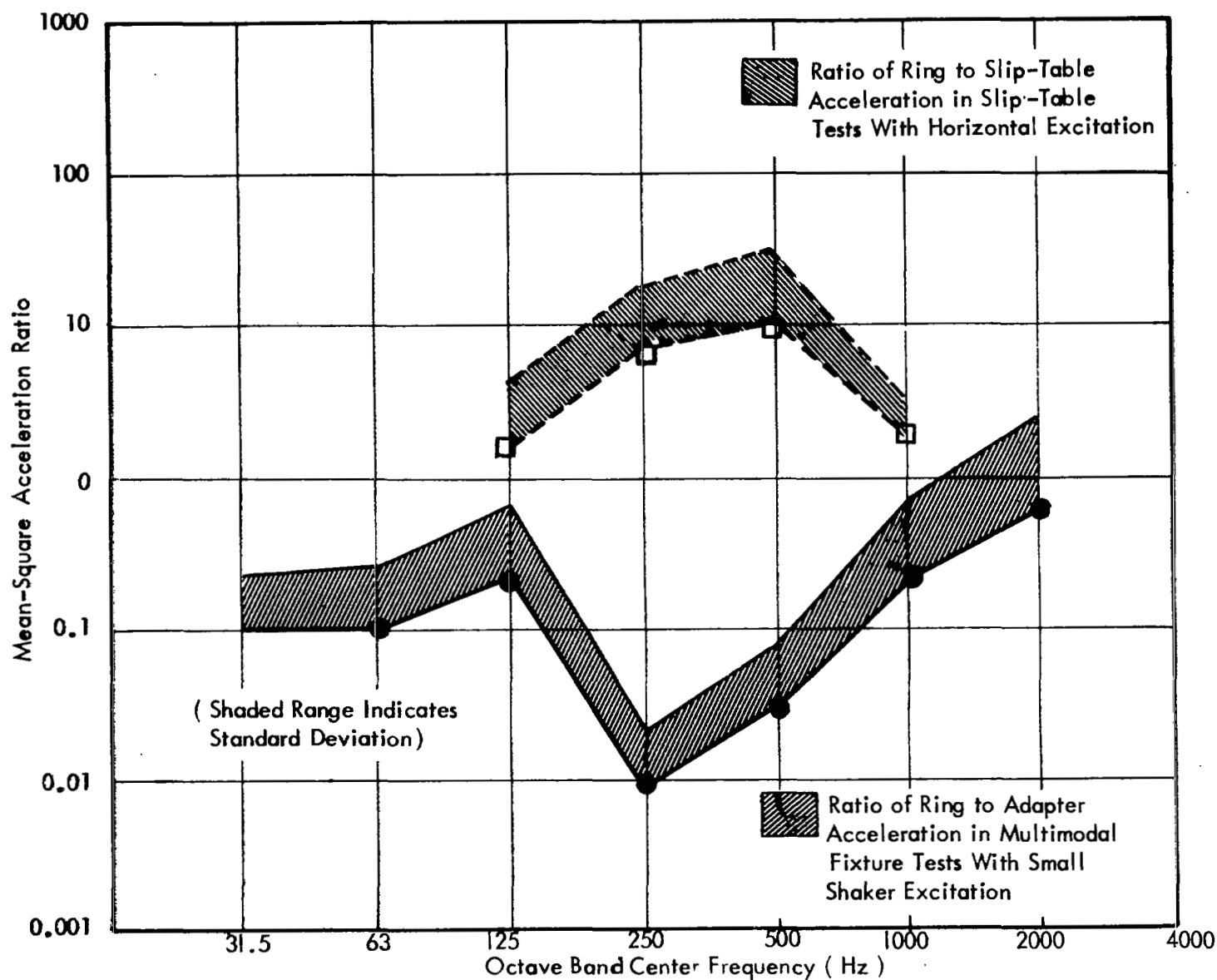


FIGURE 19. AVERAGE TRANSFER FUNCTIONS FROM ADAPTER AND SLIP-TABLE TO SENSORY RING IN OCTAVE BAND RANDOM TESTS

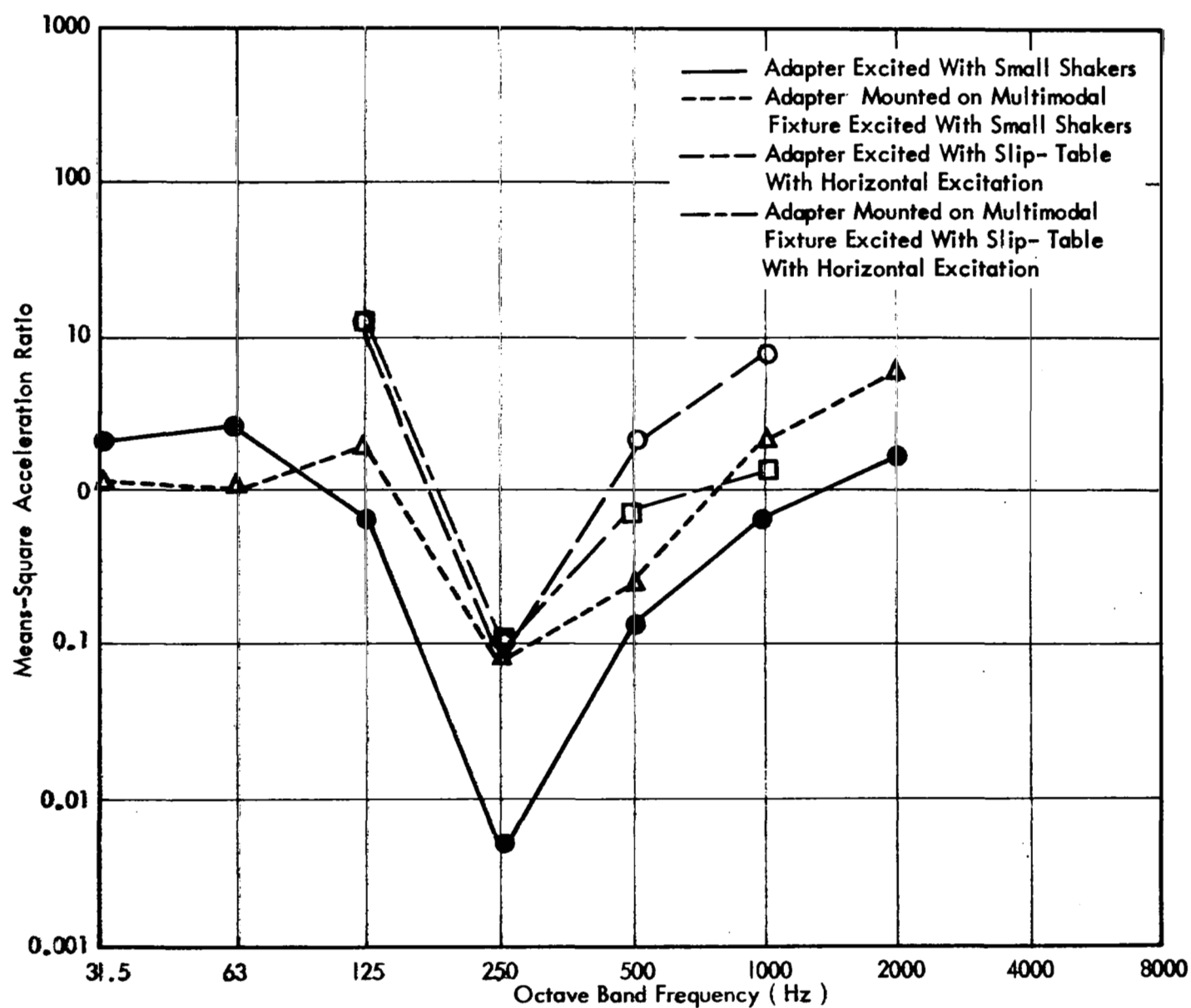


FIGURE 20. AVERAGE TRANSFER FUNCTIONS FROM ADAPTER TO SENSORY RING IN OCTAVE BAND RANDOM TESTS

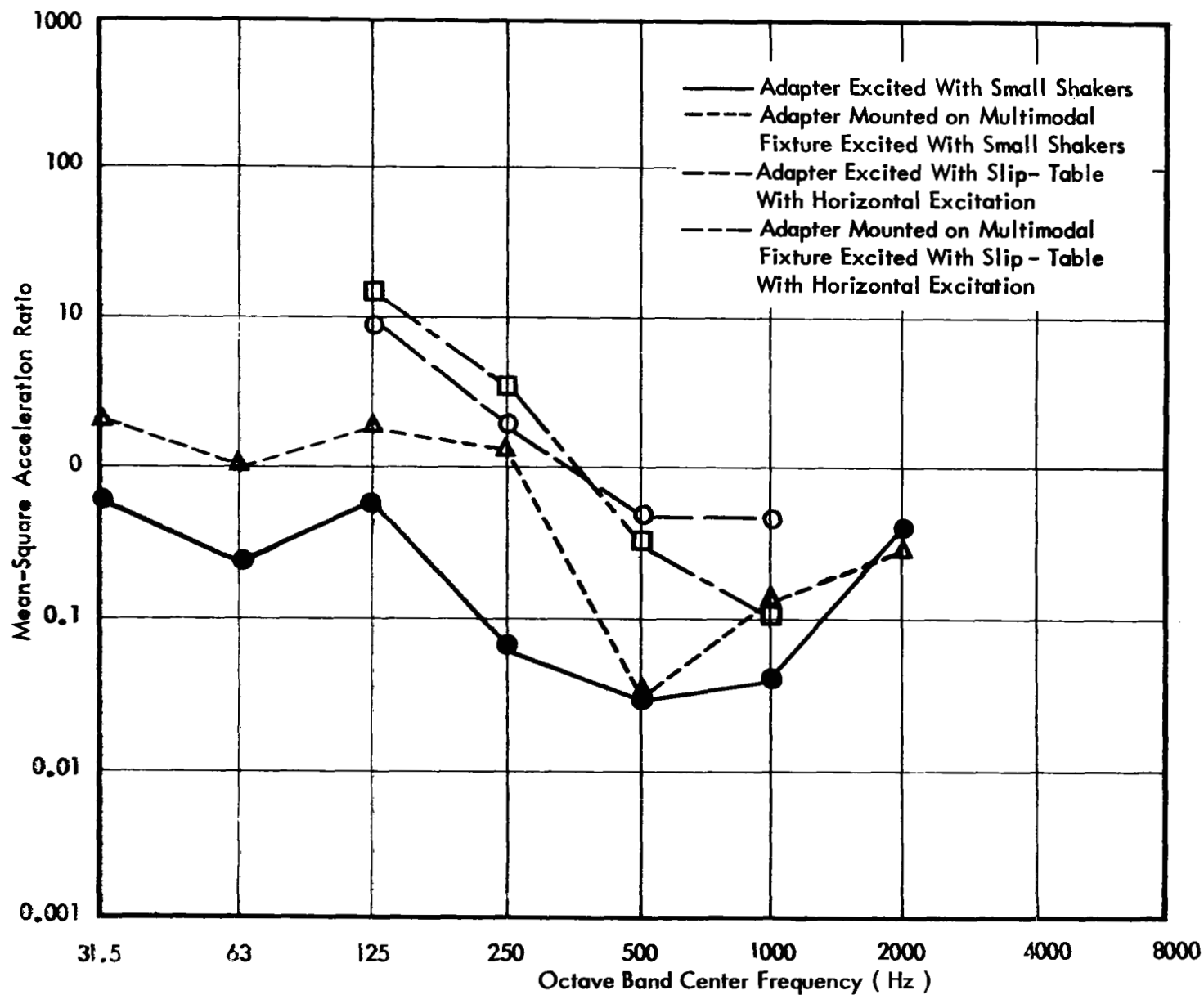


FIGURE 21. AVERAGE TRANSFER FUNCTIONS FROM ADAPTER TO CONTROL BOX IN OCTAVE BAND RANDOM TESTS

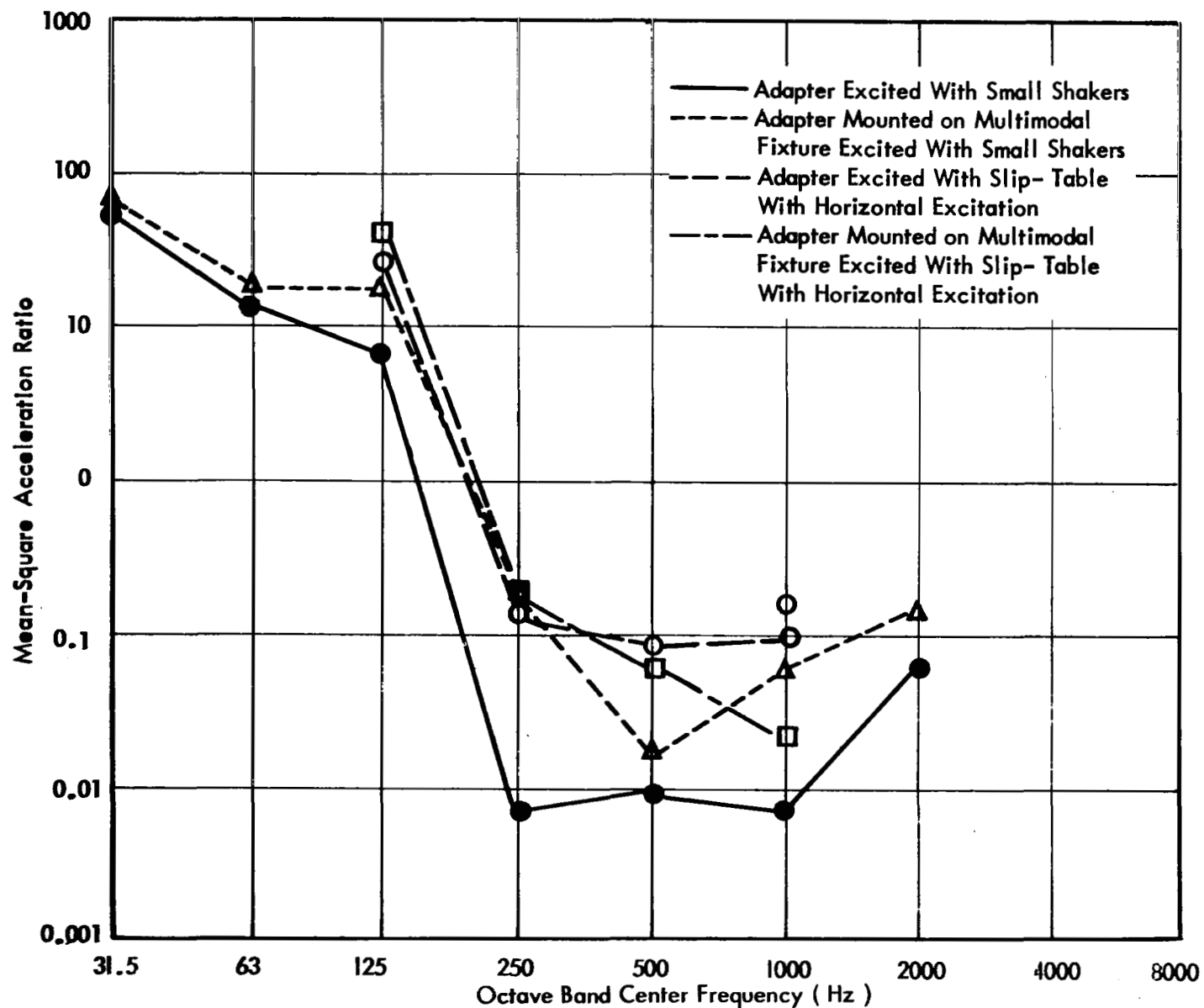


FIGURE 22. AVERAGE TRANSFER FUNCTIONS FROM ADAPTER TO SOLAR PANELS IN OCTAVE BAND RANDOM TESTS

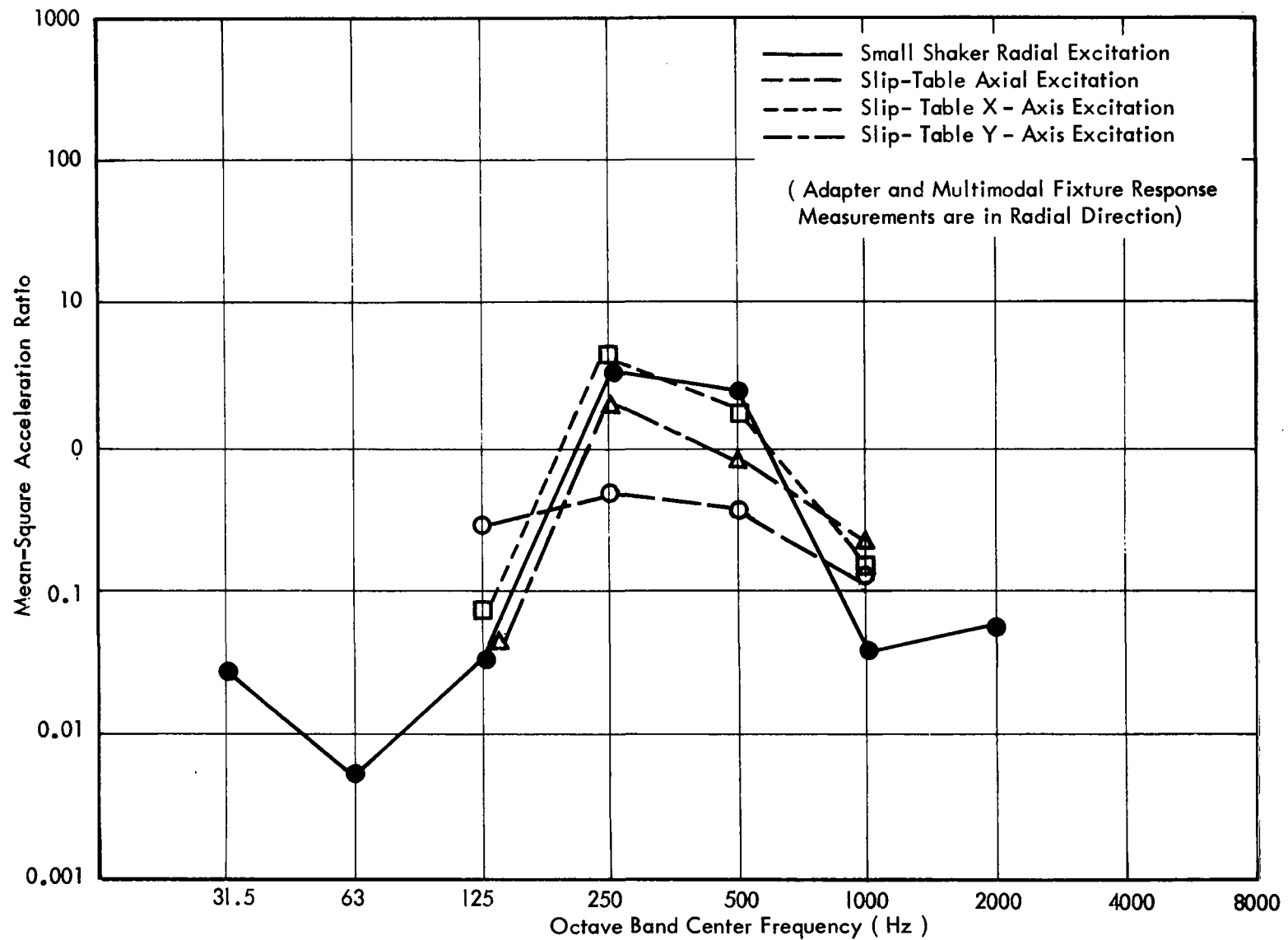


FIGURE 23. SPACE- AVERAGE TRANSFER FUNCTIONS FROM MULTIMODAL FIXTURE TO ADAPTER FOR DIFFERENT EXCITATION AXES IN OCTAVE BAND RANDOM TESTS

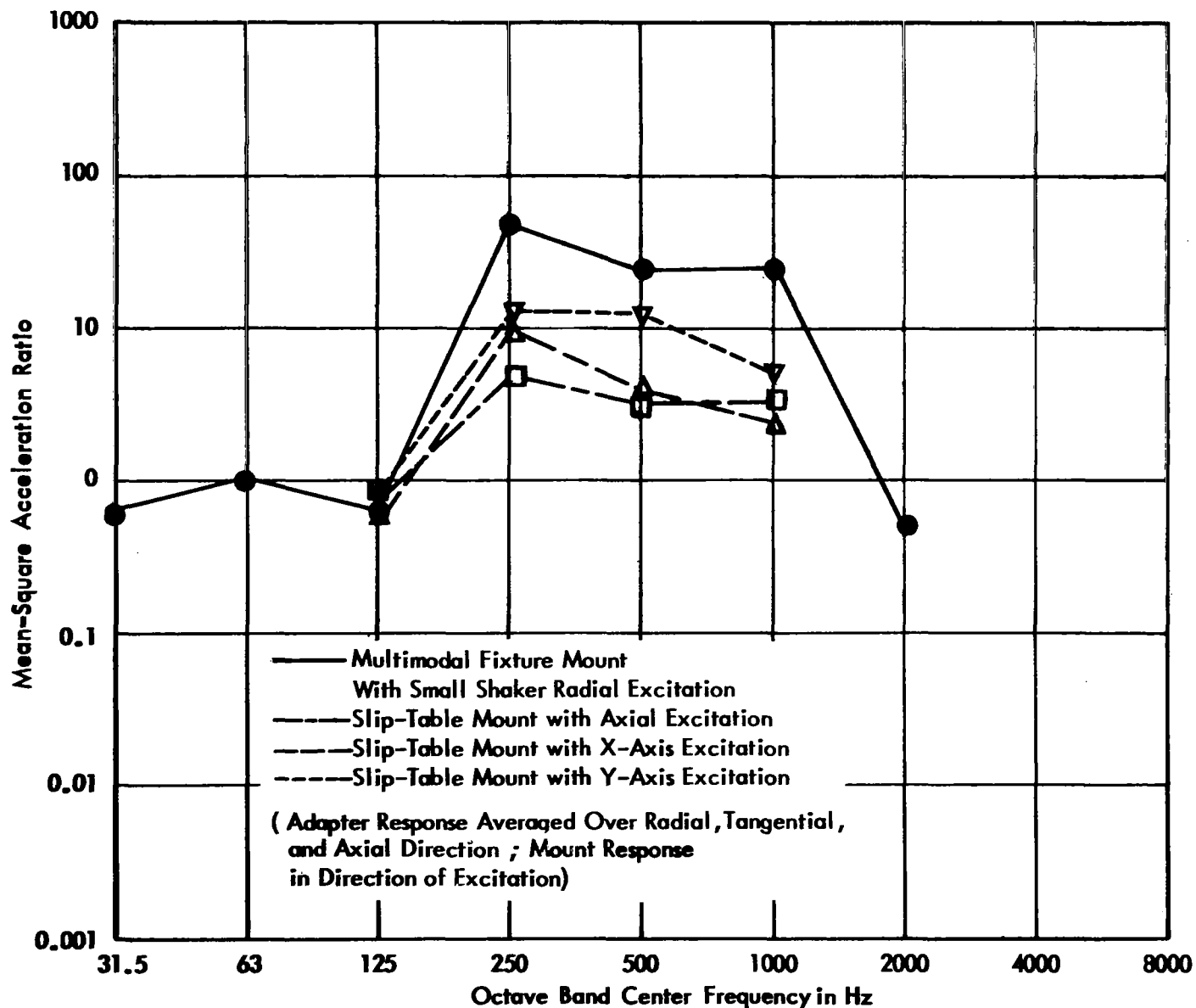


FIGURE 24. AXIS-AVERAGE TRANSFER FUNCTIONS FROM MOUNT TO ADAPTER FOR DIFFERENT EXCITATION AXES IN OCTAVE BAND RANDOM TESTS

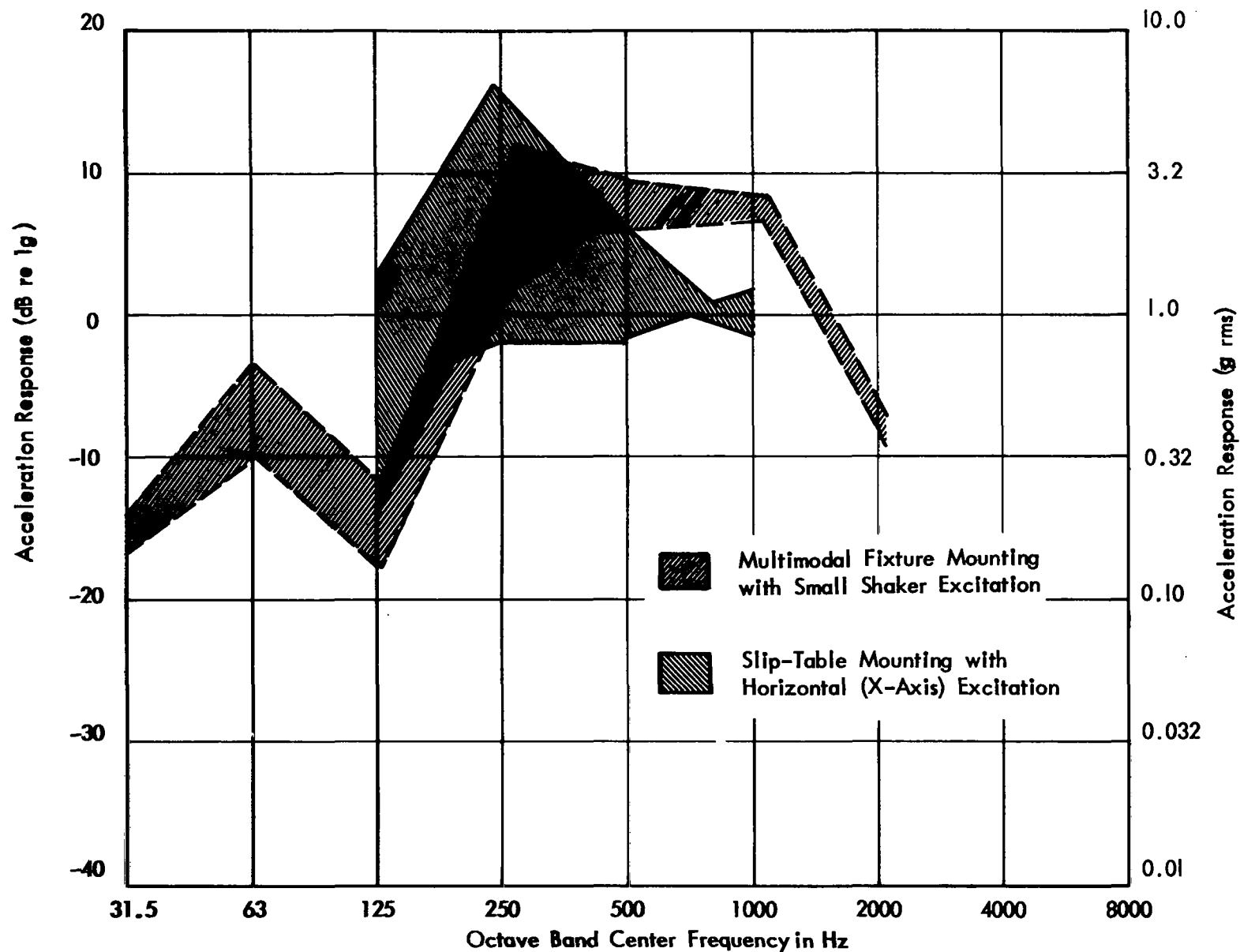


FIGURE 25. SPREAD OF RADIAL, TANGENTIAL, AND AXIAL RESPONSE MEASUREMENTS ON ADAPTER IN MULTIMODAL FIXTURE AND SLIP-TABLE MOUNT OCTAVE BAND RANDOM TESTS

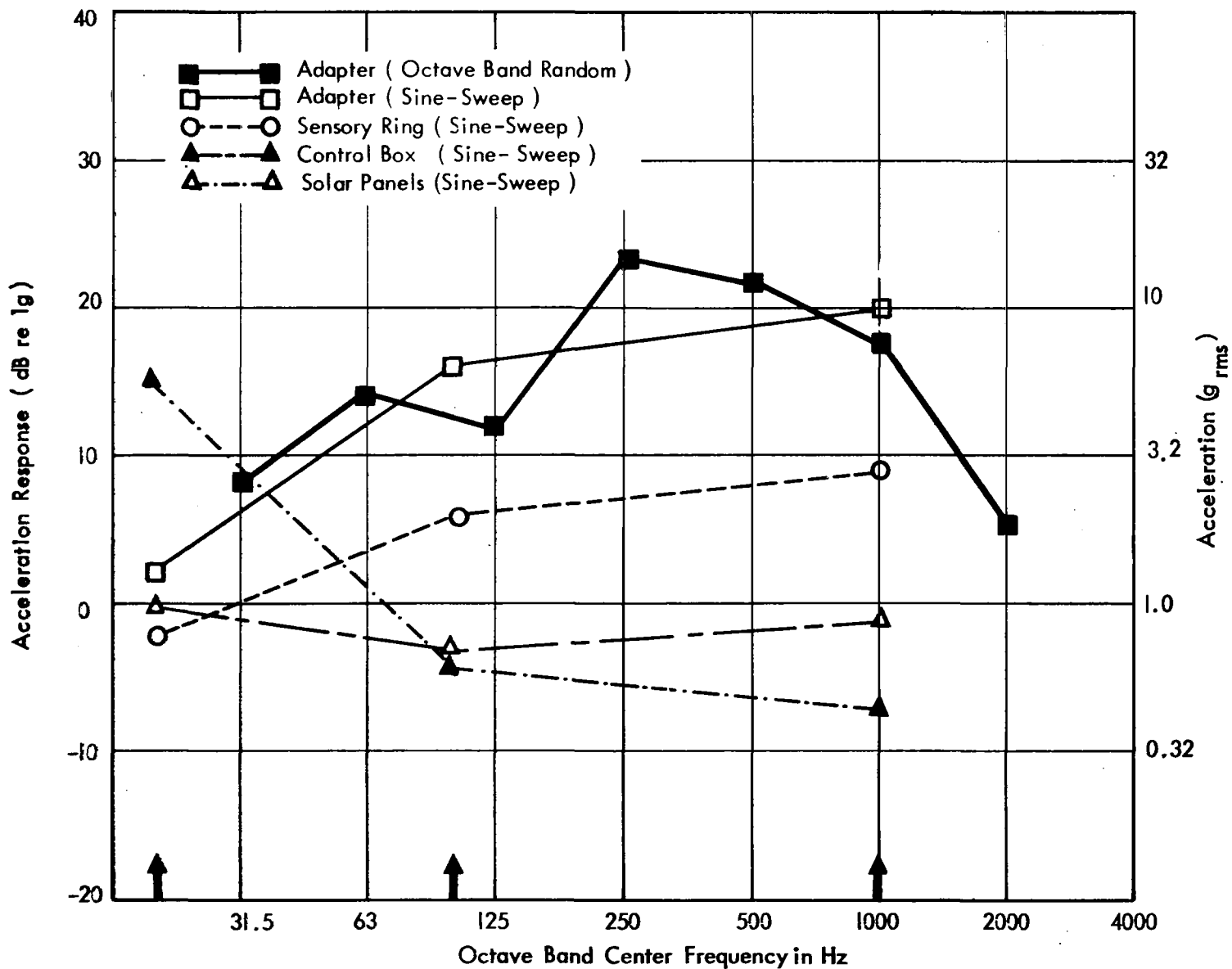


FIGURE 26. MAXIMUM ATTAINABLE ACCELERATION LEVELS WITH THREE 25 LB FORCE SHAKERS EXCITING MULTIMODAL FIXTURE

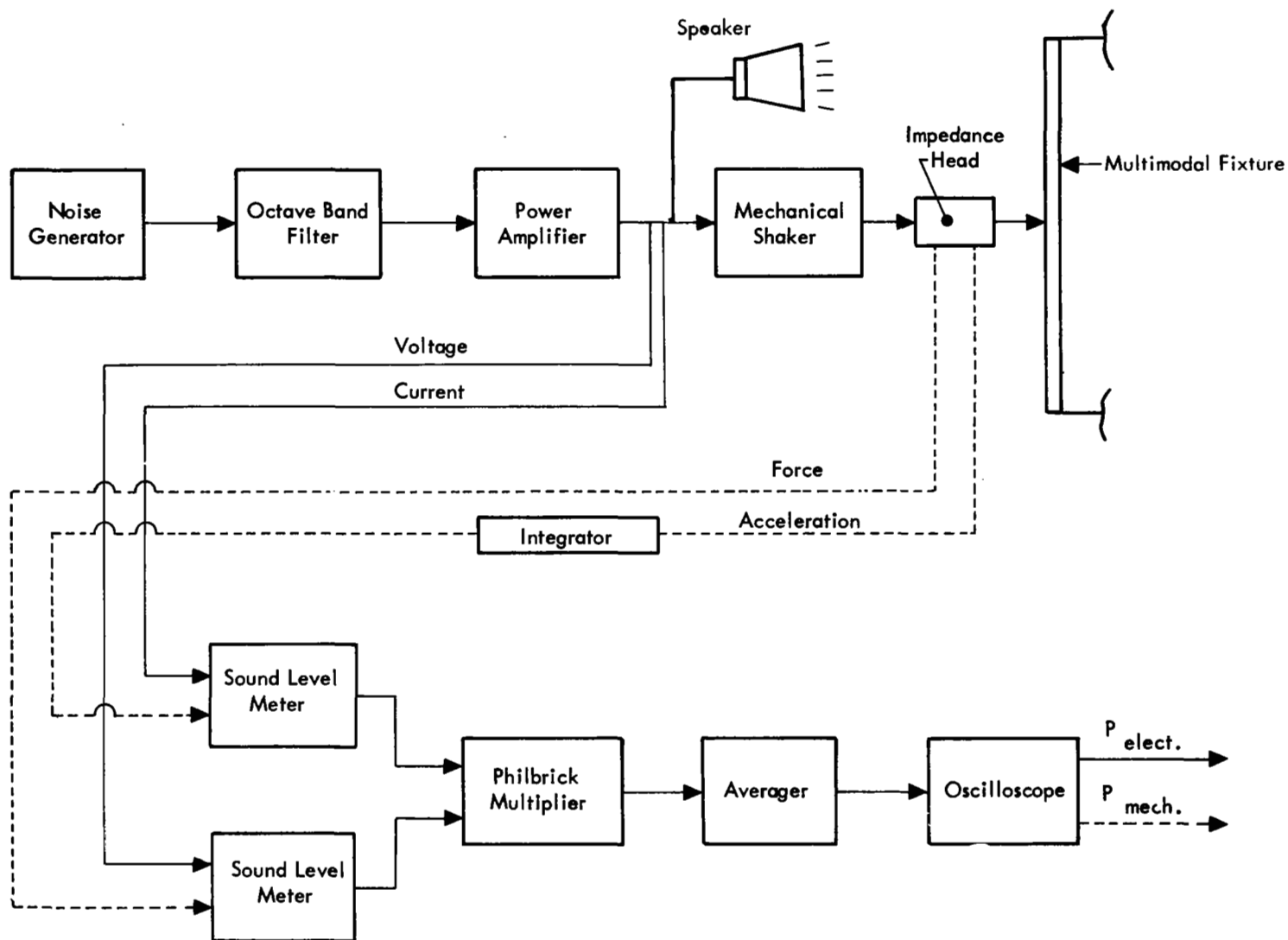


FIGURE 27. ELECTRICAL AND MECHANICAL INPUT POWER MEASUREMENT APPARATUS

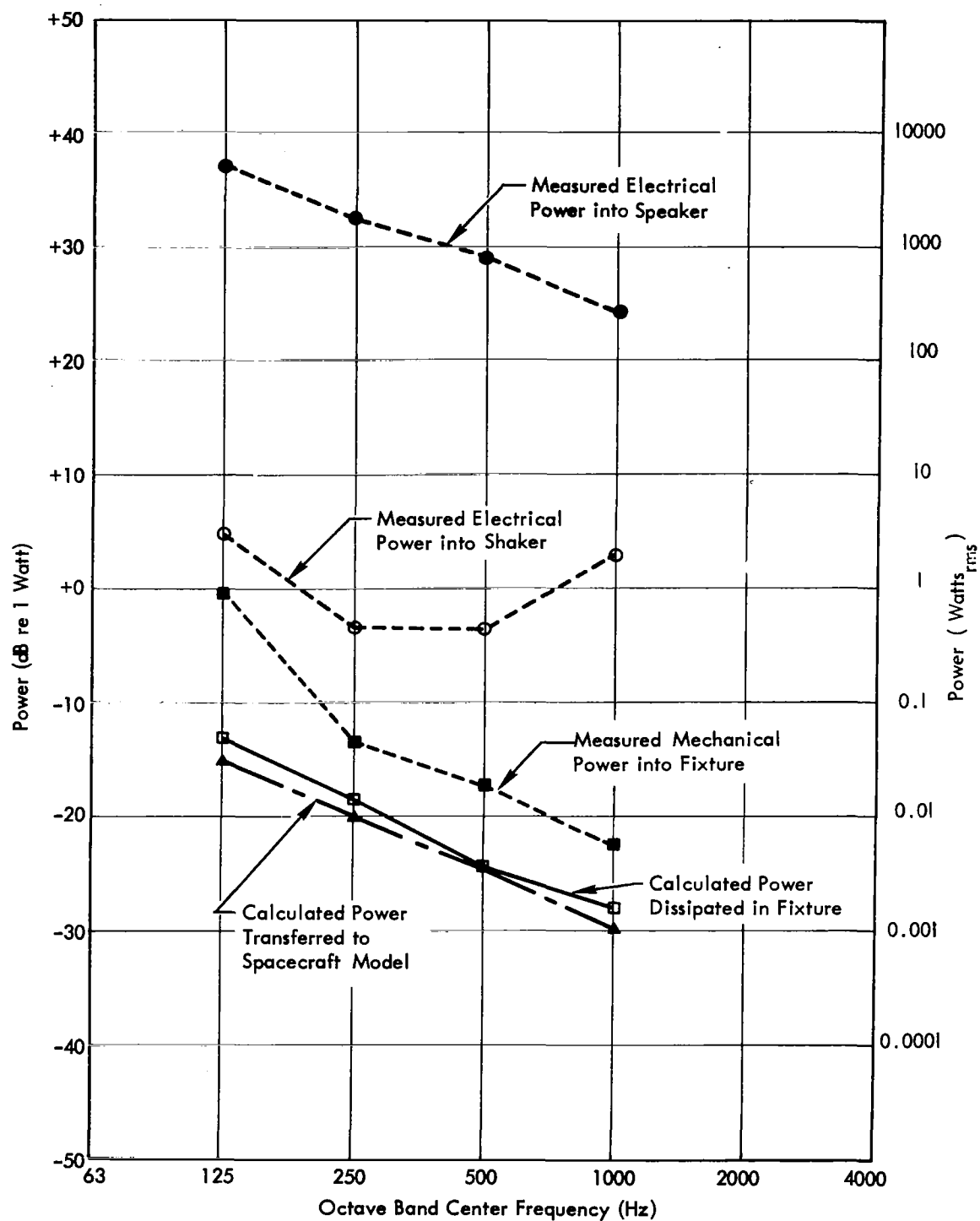


FIGURE 28. POWER MEASUREMENTS
 (All Power Quantities are Normalized for the Case of "1g"
 rms Acceleration Space-Average Fixture Response)

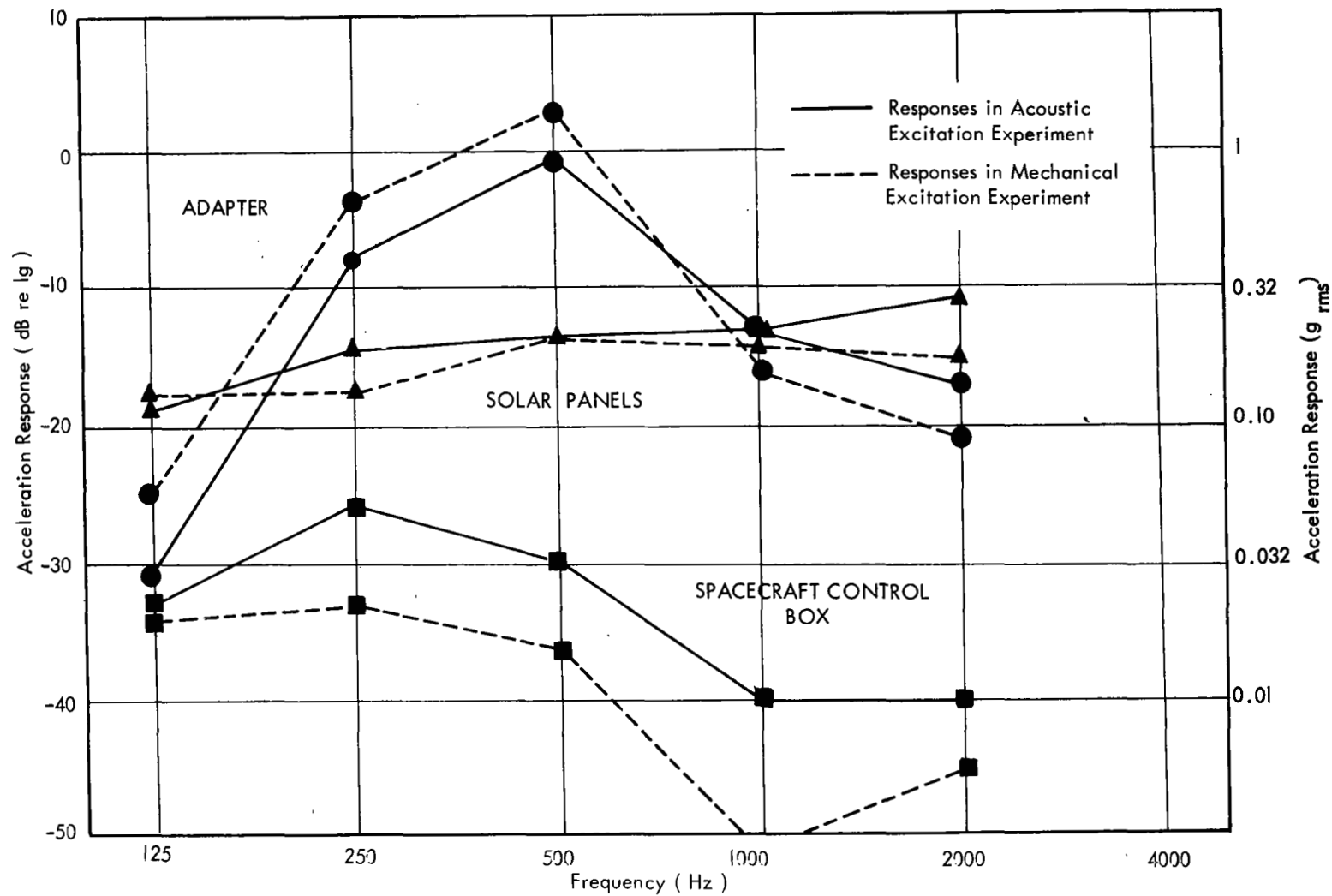


FIGURE 29. RESPONSES OF SPACECRAFT ELEMENTS IN SUBSTITUTE ACOUSTIC TESTS BASED ON INPUT POWER SIMULATION